

Rates of active compressional deformation in central Italy and Sicily: evaluation of the seismic budget

Francesco Visini · Rita de Nardis · Giusy Lavecchia

Received: 11 August 2008 / Accepted: 12 July 2009 / Published online: 5 August 2009
© Springer-Verlag 2009

Abstract Historical and recent seismicity records and available source mechanisms in eastern-central Italy (Marche–Adriatic region), in mainland-southern Sicily and in the Tyrrhenian offshore of northern Sicily show comparable deformation patterns. Seismotectonic considerations indicate that each of the three areas represents a broad seismogenic province of relatively homogeneous deformation. On the basis of the historical earthquake catalogue, the parameters of the Gutenberg–Richter distribution have been calculated by means of a Monte Carlo simulation method. The average moment tensors have been computed from focal mechanism data and the strain rate and velocity tensors evaluated by means of Kostrov's (*In Izv Acad Sci USSR Phys Solid Earth* 1:23–44, 1974) relation, which also considers the shape and size of the seismogenic volume. The uncertainties have been systematically incorporated. The results show that the three seismotectonic provinces are all undergoing shortening at seismic rates (~ 0.3 mm/year in the WSW–ENE direction in the eastern Marche–Adriatic region, ~ 0.1 mm/year in the N–S direction in mainland-southern Sicily and ~ 0.2 mm/year in the NW–SE direction in the Southern Tyrrhenian zone). The motion pattern in the Marche–Adriatic and in the Sicilian provinces suggests that these areas undergo active crust-scale deformation along reverse

shear zones, in agreement with recent horizontal GPS motion model and other independent evidence.

Keywords Seismotectonics · Active thrust faulting · Seismogenic crustal deformation · Sicily · Marche–Adriatic region · Southern Tyrrhenian Sea · Italy

Introduction

Knowledge of the velocity and strain tensors of seismogenic deformation is an essential tool for determining the seismic hazard of an active region. Geological, geodetic and seismological data may provide insights into the strain fields, and their integration is necessary in order to obtain more constrained and stable strain parameters and to improve estimates of earthquake forecast.

Geological data are capable of recording the long-term deformation history of a region and the related strain release patterns. Consequently, they may allow us to extend the history of slip of a seismogenic region to a large number of earthquake cycles (Yeats and Prentice 1996; Ward 1998; Papanikolaou et al. 2005). Obviously, the completeness of geological strain rate depends on the availability of quantitative geological data for the study area. Well-constrained data such as the 3D geometry and kinematics of the seismogenic structures, timing of the deformation, accurate displacement evaluation and slip rates are not always available (Ward 1998; Roberts 2006; Wallace et al. 2007).

Geodetic strain takes into account the total value of the active deformation, but it is unable to discriminate the seismic components from the aseismic ones. Moreover, it is still unclear whether geodetic data can be extrapolated to

F. Visini (✉) · G. Lavecchia
Laboratorio di Geodinamica e Sismogenesi, Dipartimento di
Scienze della Terra, Università “G. d’Annunzio”,
Campus Universitario, 66013 Chieti Scalo, Italy
e-mail: f.visini@unich.it

R. de Nardis
Dipartimento della Protezione Civile,
Servizio Sismico Nazionale, DPC-SSN, Rome, Italy

longer time periods owing to the short instrumental record (Papanikolaou et al. 2005).

Seismological strain has the advantage of showing the existence of sometimes still unrecognised active faults. On the other hand, owing to the limitation of the temporal windows of observation ($\sim 1,000$ years for historical seismicity and ~ 25 years for instrumental seismicity), if an earthquake had not occurred within this period, the associated structure would remain unrecognised, in the absence of other sources of information. The seismological approach remains particularly interesting in areas where quantitative geological data are missing or are insufficient to allow a detailed fault/slippage analysis.

In peninsular Italy and Sicily, seismic deformation is prevalently concentrated within a narrow extensional belt which extends along the axis of the Apennine mountain chain, from northern Tuscany to Calabria and northern Sicily (Fig. 1). Subordinate seismic activity characterises the outer thrust domains of the northern Apennines, the Calabrian–Ionian arc and mainland-southern Sicily, as well as a narrow compressional strip in the southern Tyrrhenian Sea offshore of northern Sicily (Fig. 1).

Moderate-to-large earthquakes indicate SW–NE extension perpendicular to the Apennine belt (Pondrelli et al. 2006), with average extension rates estimated from seismic moment summation of recent and historical earthquakes ranging from 1 to 3 mm/year (Anderson and Jackson 1987; Jackson and McKenzie 1988; Pondrelli et al. 1995; Selvaggi 1998) up to 5–6 mm/year (Westaway 1992). Summed geological extensional rates computed across the central Apennines range between values of ~ 2 mm/year (Visini et al. 2008) and ~ 4.0 mm/year (Roberts and Michetti 2004; Papanikolaou et al. 2005).

Whereas the geometry and dimension of the intra-Apennine extensional process are fairly well agreed in the literature, active compression at the front of the Apennine fold and thrust belt of Italy is a highly debated topic, especially in terms of spatial continuity and amplitude (Frepoli and Amato 1997; Coward et al. 1999; Finetti et al. 2001; Di Bucci and Mazzoli 2002; Savelli et al. 2002; Lavecchia et al. 2003; Vannoli et al. 2004; Pondrelli et al. 2006; Lavecchia et al. 2007a, b; Boncio and Braccone 2008).

Regional-scale focal mechanism data and borehole breakouts show active compression across the Padanian arcs and the Marche–Adriatic arc in central Italy, the Sciacca–Gela–Catania arc in mainland-southern Sicily and across the narrow E–W striking strip off the northern coast of Sicily in the southern Tyrrhenian Sea (Montone et al. 2004; Chiarabba et al. 2005; Neri et al. 2005; Jenny et al. 2006; Lavecchia et al. 2007a, b).

Seismic strain rates computed by means of scalar seismic moments from historical earthquakes and/or

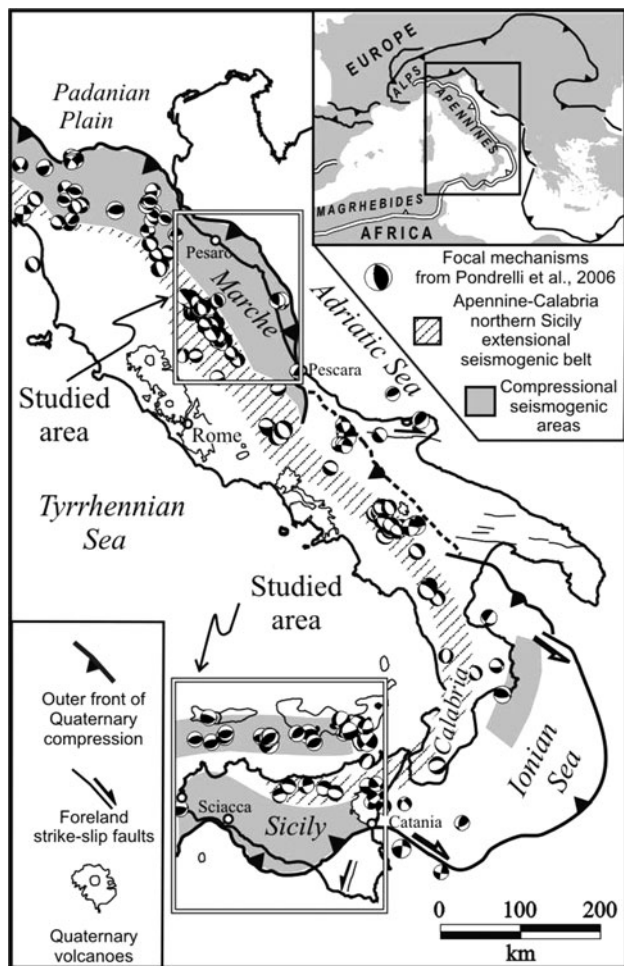


Fig. 1 Regional seismotectonic framework of the study areas, with first-order active compressional and extensional domains and major earthquake focal mechanisms ($M_w \geq 4.5$; 1977–2004). The upper inset shows the locations of Fig. 1 and schematises the outer front of the Neogene–Quaternary Apennine–Maghrebian fold-and-thrust system

summation of seismic moment tensors from instrumental events indicate a SW–NE shortening rate in the range of 0.3–0.5 mm/year along the Padanian–Adriatic arc (Westaway 1992). The seismic deformation rates computed for Sicily differ from one author to the next, showing up to fivefold difference. Kiratzi (1994) evaluated an average shortening of 1 mm/year in the NNE–SSW direction across the entire island of Sicily and its northern offshore. Jenny et al. (2006) considered separately the mainland-southern Sicily area and the Tyrrhenian offshore area and for both of them computed an average NW–SE shortening of 0.1–0.2 mm/year.

On the basis of continuous and/or survey-mode GPS data, some authors have computed active compression across the Padanian arcs in the SW–NE direction at a velocity of 0.8 mm/year (Serpelloni et al. 2005), across the Marche–Adriatic arc in the SW–NE direction at a velocity of 1.6 mm/year (Devoti et al. 2008), across mainland-

southern Sicily in the NW–SE direction at ~ 3 mm/year (Ferranti et al. 2008) and across the southern Tyrrhenian strip in the NW–SE direction at ~ 2 to 4 mm/year (Jenny et al. 2006; Serpelloni et al. 2007).

The aim of our study is to provide an evaluation of the seismic deformation budget over a period of nearly 400 years for the active compressional domains of central Italy (Marche–Adriatic area) and of Sicily (offshore and onshore), where active shortening evaluation from geological data is difficult and continuous geodetic observation exists only for the last decade, with a non-optimal network configuration (RING, Selvaggi 2006; IGFN, Vespe et al. 2000). Computed seismic strain rate and velocity tensors will allow us to compare the three study areas in terms of seismogenic activity and will give a term of comparison with the deformation budgets computed with different methodological approaches, highlighting the possible gap in seismic release with respect to the overall seismogenic potential. We will adopt a procedure which takes into consideration both geological and seismological data input (Papazachos and Kiratzi 1992). The earthquake data have been derived from two datasets. The first one, used for the computation of the moment magnitude relations, consists of a list of $M_w \geq 4.5$ historical events; the second one, used to get the tensor components, consists of a compilation of the available fault plane solutions of major and minor earthquakes. Geometric parameters of the seismogenic volumes involved in the deformation have been assumed from previous papers (Lavecchia et al. 2007a, b), where they had been derived from an integrated analysis of geological, geophysical and seismological data.

Seismotectonic framework

In the last 25 years, three well-known seismotectonic zonings of the Italian territory have been elaborated in the frame of three national multidisciplinary research projects: *Progetto Finalizzato Geodinamica* developed in the early 1980s (Working Group GNDT 1982), *Gruppo Nazionale per la Difesa dei Terremoti* developed in the early 1990s (Scandone et al. 1992; Meletti et al. 2000; Scandone and Stucchi 2000) and *INGV-DPC-Redazione della Mappa di Pericolosità Sismica* developed in the early 2000s (Working group MPS 2004a; Meletti et al. 2008). The corresponding elaborated seismic source models are known in the Italian scientific community as ZS-PFG, ZS4 and ZS9, where ZS stands for *Zonazione Sismotettonica*. The common methodological approach has been the kinematic one; this means that the boundaries of the seismic zones correspond to the surface projection of kinematically homogeneous, active, domains defined on the basis of a cross-correlation of structural–geological data and 3D

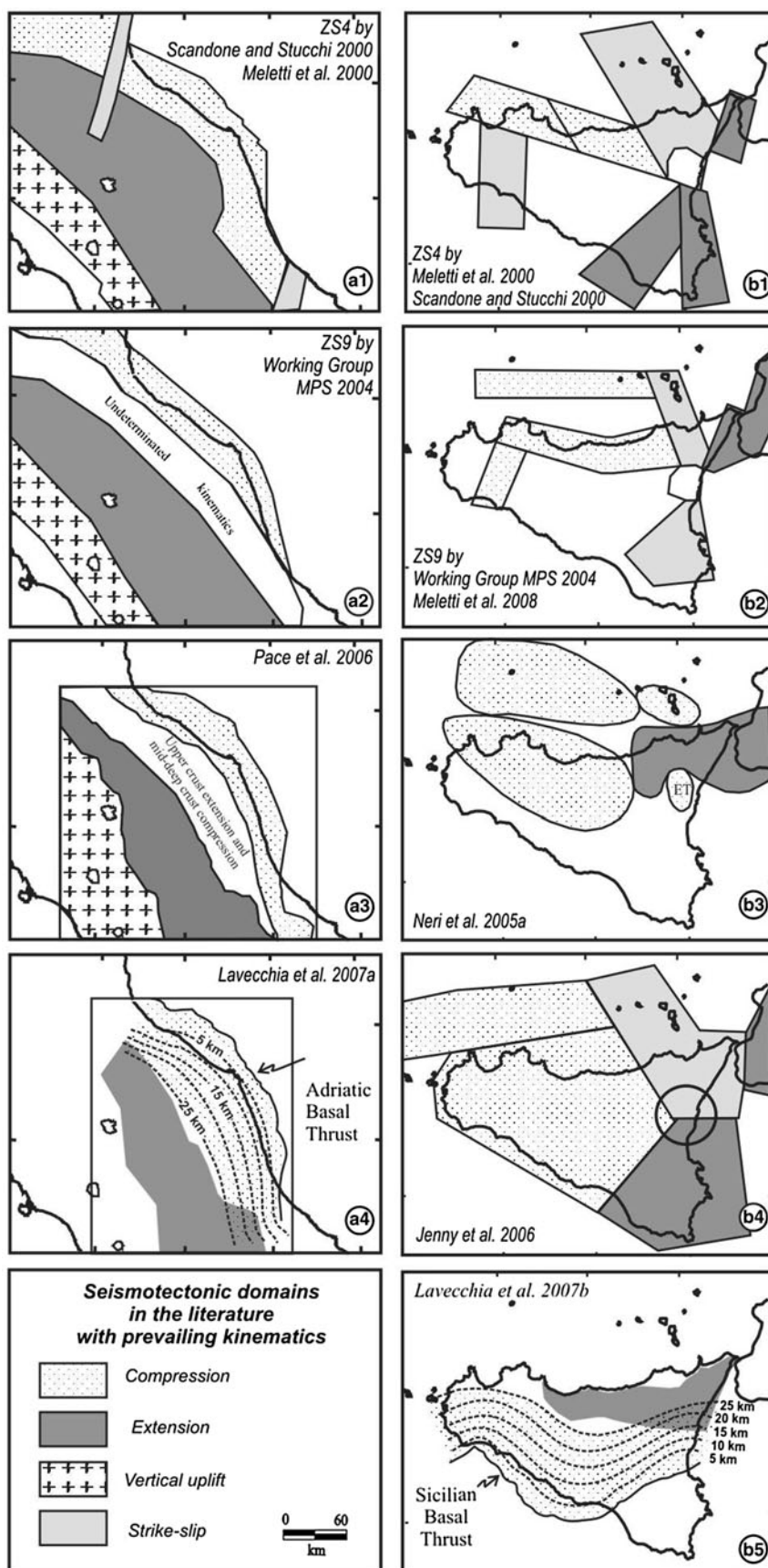
earthquake distribution data, also integrated with kinematic data referring to the long-term (generally the last 6 Ma) history of geological deformation.

Cristofolini et al. (1985) and Lavecchia et al. (1994) stressed the importance of such a 3D stress-field insight into the definition of the seismotectonic domains for Sicily and for Central Italy, respectively. They all interpreted the present seismicity in the frame of a progressive long history of deformation characterised by the outward migration, with time, of the thrust belt foredeep system, synchronous to that of the coaxial extensional domain extension in the rear. This contraction–extension pair is still active today, as witnessed by the coexistence of seismogenic extension in the Apennines and northern Sicily and of seismogenic compression along the Padanian–Adriatic and Sicilian outer thrust systems.

The seismotectonic zones proposed in the course of the years by various authors for central Italy have remained substantially unchanged (Fig. 2a and references therein). Four zones, elongated in an average NW–SE direction, are delineated from west to east. They are the Tuscan–Latium thinned crust province with a very low extensional seismicity, the highly seismogenic intra-Apennine province which is undergoing SW–NE extension, the moderately seismogenic piedmont–Apennine province which is undergoing SW–NE contraction at mid-deep crust level and the Marche–Adriatic coastal province, which is undergoing upper crust contraction. The latter is characterised by active folds, thrusts and strike-slip faults nucleated since middle Pliocene times.

More controversial is the situation for Sicily, where substantially different zonations have been proposed year by year. At the beginning (Barbano et al. 1979; Working Group GNDT 1982), the main traits of the Sicilian zonation consisted of three seismotectonic zones running roughly east–west and corresponding, from north to south, to the northern Sicilian active extension domain, to the mainland Sicilian active compressional domain, and to the active foredeep and foreland domains. Subsequently, (Fig. 2b1) in northern Sicily the E–W extensional zone was substituted by a WNW–ESE transpressional zone and mainland Sicily was interpreted as a completely aseismic domain. In western Sicily, a N–S strike-slip zone (Michetti et al. 1995), which would accommodate a differential foreland flexure retreat, was identified and was considered responsible for the Belice event in 1968. In addition (Fig. 2b2), an E–W zone undergoing N–S compression was identified off the northern coast of Sicily (Working group MPS 2004b). More recently, (Fig. 2b4, b5), a large domain undergoing nearly N–S compression across mainland and southern Sicily was identified by Jenny et al. (2006), based on geodetic–seismological data, and by Lavecchia et al. (2007a), based on geological–seismological data.

Fig. 2 Seismotectonic zonations proposed for central Italy (left column) and for Sicily (right column) over the course of the last 25 years, with their prevailing faulting kinematics predicted on the basis of integrated seismological and geological analysis. ZS Zonazione Sismotettonica; **a1, b1** zonation known as ZS4, defined in the frame of the 1996–1999 GNDT (Gruppo Nazionale Difesa Terremoti) research project; **a2, b2** zonation known as ZS9, defined in the frame of INGV-Protezione Civile Redazione della Mappa di Pericolosità Sismica (2003–2004); **a3** geologically controlled seismotectonic provinces defined for seismic hazard purposes; **b3** homogeneous seismotectonic domains based on the detailed analysis of microseismic fault plane solutions; **a4, b5** extensional and compressional provinces with contour depth lines of the seismogenic basal thrust; **b4** large-scale seismic source zones with homogeneous seismotectonic regime and comparable seismic potential



By integrating constraints on tectonic style from seismic lines and geologic data with the traditional constraints from historical and instrumental seismicity catalogues, Lavecchia et al. (2007a, b) have interpreted both the mainland-southern Sicily and the Marche–Adriatic seismotectonic provinces as corresponding to active deformation volumes at the hanging-wall of inward-dipping regional-scale basal thrusts named, respectively Sicilian Basal Thrust (SBT) and Adriatic Basal Thrust (ABT) (Fig. 2 a4, b5). Both the SBT and the ABT could penetrate the entire crust to a depth of at least 25 km with an average dip of nearly 25–30°. In both regions, the thickness of the seismogenic layer deduced from seismic data coherently deepens inward from shallow depths to mid and lower crustal depths well supporting such a configuration. Therefore, in a 3D view the Adriatic and Sicilian provinces may be schematically represented as crust-scale wedge-shaped seismogenic volumes. In map view, the two provinces correspond to arc-shaped, outward convex polygons, whose boundaries coincide with the map-view thrust front trajectory and with the surface projection of the basal thrust 25 km depth contour line.

More complicated and highly questionable are the geometry and nature of the seismogenic structures responsible for the E–W seismic belt of the Southern Tyrrhenian, where a relevant component of the Europa–Nubia NW–SE convergence is considered to be accommodated (D’Agostino and Selvaggi 2004; Goes et al. 2004; Pondrelli et al. 2004; Serpelloni et al. 2005). Such a compressional strip began its activity in Late Pleistocene times (Goes et al. 2004), inverting the pre-existing extensional structures of the thin-crust Tyrrhenian domain. Some authors (Jenny et al. 2006) associate the seismic activity with a north-verging back thrust developed at the hanging-wall of the subduction plane which dips northward beneath Sicily and the Tyrrhenian Sea and emerges along the south Sicily thrust front. Other authors (Chiaramba et al. 2005; Serpelloni et al. 2005) hypothesise a south-verging thrust which would represent the active front of the compressional deformation between the Nubia and European plates now shifted nearly 150 km northward with respect to the former, now abandoned, southern Sicily front of the Apennine–Maghrebian compressional belt. Others (Billi et al. 2007) assume a general southward vergence of the belt and associate it with an incipient flip of the subduction plane, hypothesising a south-dipping subduction of the oceanic Tyrrhenian crust beneath Sicily.

An open fundamental question in the seismotectonic interpretation of Sicily involves the spatial and geometric relations between the Southern Tyrrhenian and the mainland-southern Sicily compressional provinces. According to some authors (Kiratzi 1994; Jenny et al. 2006), the two are in physical continuity and undergo a common coaxial

compression. According to others (Neri et al. 2005; Lavecchia et al. 2007a, b), a nearly E–W striking extensional seismogenic domain is interposed between the two. This last point of view is supported by the presence in the Peloritani and Nebrodi–Madonie areas of northern Sicily of a neat belt of extensional focal mechanisms, which are in continuity with the Apennine and Calabria extensional seismic belt (Pondrelli et al. 2006).

In the current paper, we will adopt this last point of view and will compute the corresponding pattern and rate of deformation, separately.

Procedure

In order to estimate the velocity tensor representative of the active deformation within the Marche–Adriatic, mainland-southern Sicily and Southern Tyrrhenian seismotectonic provinces, we have used the procedure proposed by Papazachos and Kiratzi (1992), integrating analyses of seismological data and geological information referring to the geometry of the deformed volume. This procedure requires not only knowledge of complete historical and instrumental records over a certain magnitude threshold and of the associated Gutenberg–Richter (G–R) parameters, but also knowledge of the shape and size of the seismogenic volume, as well as that of the kinematics of the active deformation deduced from reliable fault plane solutions.

The procedure is articulated in the following steps:

- computation of the scalar seismic moment rate (\dot{M}_o) from historical and instrumental earthquakes,
- computation of the moment tensor (\bar{F}_{ij}) from focal mechanism data,
- computation of the average seismic strain rate tensor ($\dot{\epsilon}_{ij}$),
- computation of the components of the velocity tensor (U_{ij}),
- evaluation of the errors which may be involved in the above computations.

The scalar seismic moment rate (\dot{M}_o) within each seismogenic volume in the years of the completeness interval may be calculated by means of Molnar’s (1979) relation:

$$\dot{M}_o = \frac{A}{1-B} M_{o\max}^{1-B} \quad (1)$$

where $A = 10^{[a+(bd/c)]}$, $B = \frac{b}{c}$, a and b are values of the Gutenberg–Richter relation, $M_{o\max}$ is the scalar moment of the largest observed earthquake in the region, $M_o = 10^{c \times M_s + d}$, c and d are constants of the moment–magnitude relation (Kanamori and Anderson 1975). The advantage of

this formula is that the full record of seismicity in any given region can be used, the a and b values of the Gutenberg–Richter relation being the most important parameters in this calculation.

The focal mechanism moment tensor (\bar{F}_{ij}), which is a function of strike, dip and rake of the fault plane solutions, may be derived from the calculation of an average focal mechanism starting from the available focal mechanism dataset.

The average seismic strain rate tensor ($\dot{\epsilon}_{ij}$), which is the symmetric part of the velocity gradient tensor may be calculated by means of Kostrov's (1974) relation:

$$\dot{\epsilon}_{ij} = \frac{1}{2\mu V} \dot{M}_o \bar{F}_{ij} \quad (2)$$

where V is the volume of the seismogenic deforming region and μ is the rigidity modulus. In the general case, the seismogenic volume V may be derived from the length (l_1), width (l_2) and the average thickness of the seismogenic layer (l_3).

The components of the velocity tensor U_{ij} may be calculated with the formula developed by Jackson and McKenzie (1988):

$$U_{ii} = \frac{1}{2\mu l_k l_i} \dot{M}_o \bar{F}_{ii} \quad \text{with } i = 1, 2, 3, \text{ and } k \neq i, i \neq j, j \neq k \quad (3)$$

$$U_{i2} = \frac{1}{2\mu l_1 l_3} \dot{M}_o \bar{F}_{12} \quad (4)$$

$$U_{i3} = \frac{1}{2\mu l_1 l_2} \dot{M}_o \bar{F}_{i3} \quad \text{with } i = 1, 2 \quad (5)$$

These equations are valid on the condition that l_3 is much smaller than l_1 and l_2 , and l_1 is much greater than l_2 . The reference system in Eqs. 2–5 is the province's local system (length/width/depth). Since \bar{F}_{ij} is usually calculated in the north/east/down system, a rotation in the local province's system is necessary.

The possible errors involved in the calculation of the above equations are clearly controlled by errors in \dot{M}_o , while the directions of the eigenvectors of the deformation are mainly influenced by errors in the focal mechanism tensor (e.g. in F) (Papazachos and Kiratzi 1992).

As evident from Eq. 1, errors in \dot{M}_o may derive from errors in the a , b , c , d values and in the choice of the M_{\max} and in the adopted M_s – M_o relationship. Use of the Monte Carlo simulation method and assumption of random errors in these parameters, with known medians and standard deviations, means that Gaussian deviates can be introduced. If m is the vector of mean values of the parameters, the new parameter vector $P = (a, b, c, d, M_{\max})$ can be iteratively obtained by using:

$$P = Cz + m \quad (6)$$

where z is the standard Gaussian random vector, with deviates produced with the polar Box–Mueller transform, C is the Cholesky decomposition of the covariance matrix of the parameter vector V (symmetric and positive definite matrix), with a unique lower triangular matrix such that $V = C \times C^T$.

Input data

The application of the above procedure to any homogeneous seismotectonic province requires knowledge of the shape and size of the seismogenic volume, possibly deduced from integrated geological–seismological constraints, the moment tensor deduced from reliable fault plane solutions, the values of the Gutenberg–Richter parameters and of the scalar seismic moment rate deduced from the most possible complete record of historical and instrumental earthquakes over a certain magnitude threshold.

Dimension and geometry of the seismogenic sources

In order to parameterise the dimensions (length l_1 , average width l_2 , average thickness l_3) and the azimuth with the north of each deforming seismogenic volume, we have assumed and schematised the 3D geometry given by Lavecchia et al. (2007a, b) for the Marche–Adriatic and the mainland-southern Sicily seismotectonic provinces (Fig. 2a, b, b5), whereas for the Southern Tyrrhenian province we have used the surface boundary and the average seismogenic thickness given by DISS3.0.4 (available online from <http://legacy.ingv.it/DISS/>).

By integrating constraints on tectonic style from seismic lines and geologic data with the traditional constraints from historical and instrumental seismicity catalogues, Lavecchia et al. (2007a, b) have interpreted the mainland-southern Sicily and the Marche–Adriatic seismotectonic provinces as corresponding to active deformation volumes at the hanging-wall of an inward-dipping regional-scale basal thrust, named SBT and ABT, respectively (Fig. 2a4, b5), which penetrate the crust to a depth of at least 25 km with an average dip of nearly 20–25°. In both regions, the thickness of the seismogenic layer deduced from seismic data coherently and slowly deepens from shallow depths to mid and lower crustal depths, well supporting such a configuration (Parolai et al. 2001; Lavecchia et al. 2007b). Therefore, in a 3D view, the Marche–Adriatic and the mainland-Sicily provinces, also named ABT and SBT provinces, may both be schematically represented as crust-scale wedge-shaped seismogenic volumes (Fig. 5). In map view, the two provinces correspond to arc-shaped, outward

convex, polygons whose vertices coordinates are given in Fig. 5. The eastern ABT and the southern SBT boundaries simply coincide with the corresponding thrust front, whereas the western ABT and the northern SBT boundaries correspond to the surface projection of the 25 km depth contour line of the underlying basal thrust. The ABT province, as drawn in Fig. 5, has a surface areal extent of nearly 14.400 km² with an along-strike extent (l_1) of ~240 km, measured along the thrust front and an average width (l_2) of ~60 km. The SBT province has a surface areal extent of nearly 16.200 km² with l_1 , measured along the thrust front, of ~270 km and l_2 ~60 km. Given the wedge shape of both seismogenic volumes, controlled by the deepening of the underlying basal thrust from near the surface to a depth of at least 25 km, an average vertical extent (l_3) equal to 12.5 km, may be reasonably assumed for both seismogenic volumes.

The Southern Tyrrhenian Compressional (STC) province, as drawn in Fig. 5, has a total areal extent of nearly 13.000 km² with an E–W length (l_1) of ~260 km, and an average width (l_2) of ~50 km. We do not have any geologic constraint on the maximum depth of the province. Exclusively, based onto the earthquake depth distribution data (Castello et al. 2005) an average l_3 value of 20 km has been assumed in the forthcoming calculations.

Fault plane solutions

We selected all the focal mechanisms available in the literature for the events with moment magnitudes $M_w \geq 4.0$ which occurred in the time interval 1968–2006 within the three studied areas (Fig. 3; Table 2). In the Marche–Adriatic area, prevailing strike-slip kinematics characterise the 1972 Ancona seismic sequence (M_w 4.8, Gasparini et al. 1985), whereas prevailing reverse solutions are typical of the 1987 Porto S. Giorgio sequence (M_w 4.6, Riguzzi et al. 1989) and of the remaining selected events. In any case, all the mechanisms show nearly-horizontal NE–SW to E–W trending P axes.

In Sicily, there are significantly different interpretations of the focal mechanism of the highly destructive 1968 Belice seismic sequence (M_w 5.5 in Anderson and Jackson 1987; M_w 5.6 in Morelli and Pondrelli 1998). Some authors evaluate it as right lateral transpression on a NNE-striking plane (McKenzie 1972; Gasparini et al. 1985), others as pure thrusting on north-dipping planes (Anderson and Jackson 1987) or as oblique thrusting on a north-dipping plane (Morelli and Pondrelli 1998). In all cases, even if data are not clear enough, the average P axis was nearly N–S and sub-horizontal. The few other selected events in central and eastern Sicily show reverse-oblique and strike-slip kinematics with NNW–SSE to

NNE–SSW striking P axes (Fig. 3b). Fault plane solutions, which indicate a dominant nearly N–S regional compression, are available for some minor earthquakes ($M \leq 3.6$) recorded beneath the western side of Mt Etna at depths between 10 and 30 km (see inset in Fig. 3) (Neri et al. 2005). N–S seismogenic compression was recognised in central and western Sicily, as well (Caccamo et al. 1996).

In the Southern Tyrrhenian province, the 2002 Palermo sequence shows reverse faulting on E to NE striking planes, consistent with the dominant reverse faulting of the area, as highlighted by the focal mechanisms of events (Montone et al. 2004; Pondrelli et al. 2006) with similar energy recorded in recent years in the area between Ustica and the Aeolian Islands (Fig. 3).

For each province, we derived the moment tensor (\bar{F}_{ij}), which is a function of strike, dip and rake of the fault plane solutions, from the calculation of an average focal mechanism through the application of a Linked Bingham Distribution (LBD) procedure, which is the equivalent of an unweighted moment tensor summation. The overall utilised dataset of focal mechanisms is reported in Table 2 (Figs. 3a, b and references therein). They refer to moderate events ($M_w \geq 4.0$), background seismicity and minor sequences. We were forced to consider also the moderate events and even the minor ones as the studied areas have not been struck by strong earthquakes since instrumental times and, on the other hand, local, permanent and temporary stations have registered good-quality data elaborated in terms of focal mechanisms in the literature (Neri et al. 2005).

The computed average focal mechanisms show that all the provinces are mostly accommodating reverse displacement in response to a maximum sub-horizontal compression oriented approximately WSW–ENE across the ABT province, N–S across the SBT province and NW–SE across the Southern Tyrrhenian Compressional province.

Earthquake dataset

The earthquake dataset compiled for each province, with the main aim of computing the scalar seismic moment rate (\dot{M}_o), consists of all the known crustal earthquakes with $M_w \geq 4.5$ occurred since 217 bc within the surface boundary of the province. The information was extracted from the Italian Parametric Catalogue CPTI04 (Working Group CPTI 2004a), which contains information on the Italian earthquakes from 217 bc to 2002, and subordinately from other historical regional catalogues, as well as from specific papers on major historical earthquakes (see Table 1 for the references). Information on the instrumental events was obtained from regional and local

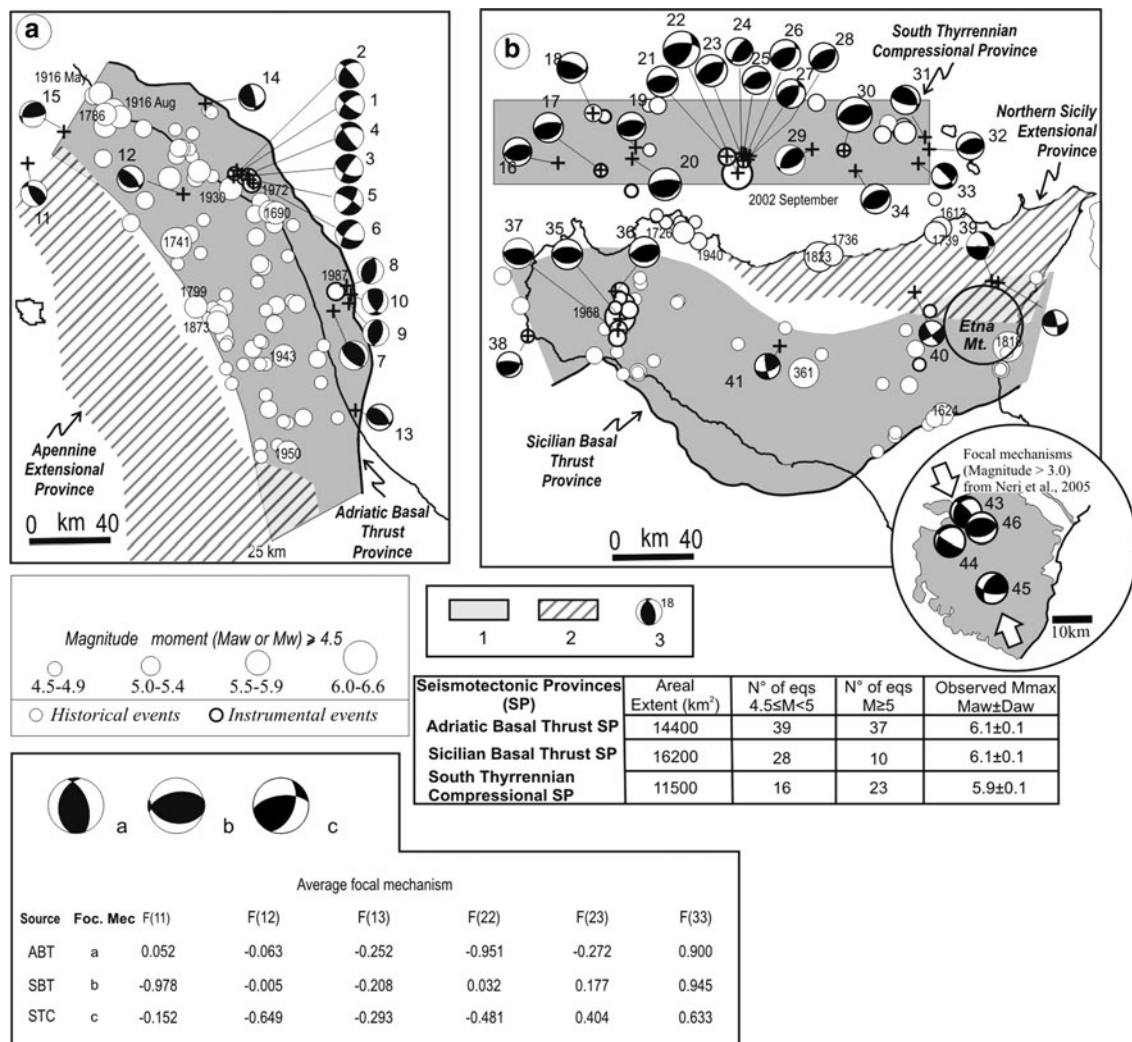


Fig. 3 Compressional seismotectonic provinces (in grey) of central-eastern Italy and Sicily, with focal mechanisms and computed average tensor components. In the maps, which are located in Fig. 1, are also represented the Apennine and northern Sicily extensional seismotectonic domains (rules) (after Lavecchia et al. 2007a). The focal mechanisms reported in the map are exclusively those falling within the boundary of the compressional province and listed in Table 2. The

central-right table reports some of the data used in the strain rate calculation; the number of earthquakes for classes of magnitude is derived from Table 1 and the maximum observed magnitude ($M_{aw} \pm \Delta M_{aw}$) is derived from the CPTI04 catalogue (Working group CPTI 2004a). In the lower-left inset, the average focal mechanism (moment tensor summation) of each province and the related moment tensor (\bar{F}_{ij}) components are reported

catalogues, as well as from some specific papers (see Table 1 for the references).

For the compilation of the earthquake–province association datasets, we selected exclusively the historical and instrumental events (Table 1), located within the province boundary in the case of the Marche–Adriatic and mainland-southern Sicily areas. The choice of the historical earthquake to be attributed to the Southern Tyrrhenian province has been much difficult. In fact, the earthquake of 6 September 2002 (M_w 5.6), located within the compressional Tyrrhenian strip about 45 km NE from Palermo at a depth range of ~5–15 km, damaged the city of

Palermo and some surrounding localities (Azzaro et al. 2004), raising an obvious question about the attribution to this province also of historical events sited along the northern coast of Sicily. Following Azzaro et al. (2004) and Jenny et al. (2006), and on the basis of the macroseismic data, we have attributed to the ST province the earthquakes which hit Palermo in 1726 (M_w 5.6), 1823 (M_w 5.9) and 1940 (M_w 5.4) (Working group CPTI 2004a). These events present very similar macroseismic features to the 2002 event, and may therefore be ascribed to larger offshore seismic sources as strongly supported by the distribution of the instrumental

Table 1 Dataset of earthquakes with moment magnitude $M_w \geq 4.5$

No.	Y	M	D	Lat	Lon	H (km)	Locality	References	I_{max}	I_o	M_{aw}	M_w
<i>Located within the boundary of the Adriatic Basal Thrust Province</i>												
1	1269	9		43.558	13.564		Ancona	DBMI04	80	80	5.6	
2	1308	1	25	44.070	12.570		Rimini	CFTI	75	75	5.4	
3	1389	4		43.837	13.018		Fano	DBMI04	70	70	5.2	
4	1472			44.059	12.567		Rimini	DBMI04	70	70	5.2	
5	1473	2	2	44.059	12.567		Rimini	DBMI04	55	60	4.8	
6	1474	8	18	43.603	13.507		Ancona	DBMI04	70	70	5.2	
7	1480			42.919	13.835		Monteprandone	DBMI04	75	75	5.4	
8	1502	9	6	43.462	13.087		Cupramontana	DBMI04	70	70	5.2	
9	1540	4	8	43.160	13.716		Fermo	DBMI04	65	65	5.0	
10	1625	12	5	44.059	12.567		Rimini	DBMI04	60	60	4.8	
11	1626	5	12	43.333	13.500		Macerata est	POS85		70	5.2	
12	1672	4	14	43.930	12.580		Riminese	CFTI	80	80	5.6	
13	1690	12	23	43.550	13.600		Anconetano	CFTI	85	85	5.7	
14	1692	10	22	43.837	13.018		Fano	DBMI04	60	60	4.8	
15	1727	12	14	43.610	12.818		S.Lorenzo in campo	DBMI04	70	70	5.2	
16	1741	4	24	43.425	13.004		Fabrianese	DBMI04	90	90	6.1	
17	1744	5	27	43.917	13.000		Medio adriatico	POS85		60	4.8	
18	1786	12	25	43.980	12.580		Riminese	CFTI	80	80	5.7	
19	1788	4	18	43.837	13.018		Fano	DBMI04	65	65	5.0	
20	1799	7	28	43.147	13.123		Camerino	DBMI04	95	90	5.9	
21	1805	5	9	43.451	13.480		Macerata	DBMI04	65	65	5.0	
22	1809	8	25	43.333	13.500		Macerata est	POS85		70	5.2	
23	1838	6	23	43.805	13.007		Pesaro	DBMI04	65	65	5.0	
24	1841	4	14	43.791	12.568		Cagli	DBMI04	65	65	5.0	
25	1870	2	8	43.550	13.471		Numana	DBMI04	70	70	5.1	
26	1873	3	12	43.080	13.250		Marche meridionali	CFTI	90	80	5.9	
27	1874	2	3	43.367	13.667		Potenza picena	POS85		60	4.8	
28	1875	3	17	44.070	12.550		Romagna sud-orient.	CFTI	80	80	5.7	
29	1882	8	16	42.979	13.875		Grottammare	DBMI04	70	65	5.0	
30	1884	1	10	42.665	13.953		Atri	DBMI04	55	55	4.6	
31	1887	5	26	43.525	13.170		Jesi	DBMI04	60	55	4.6	
32	1888	7	8	42.667	13.750		Bellante	POS85		70	5.2	
33	1895	10	25	43.167	13.700		S.Elpido a mare	POS85		60	4.8	
34	1897	9	21	43.706	12.966		Adriatico centrale	DBMI04	70	70	5.5	
35	1897	10	28	43.000	13.500		Force	POS85		55	4.6	
36	1899	6	22	43.250	13.500		Corridonia	POS85		60	4.8	
37	1900	8	10	42.650	13.650		Teramo ovest	POS85		60	4.8	
38	1901	9	25	43.833	13.000		S.costanzo	POS85		55	4.6	
39	1904	9	2	43.000	13.300		Bolognola	POS85		60	4.8	
40	1905	11	30	43.117	13.250		S.ginesio	POS85		55	4.6	
41	1906	1	29	42.767	13.533		Castel trosino	POS85		55	4.6	
42	1907	1	23	42.819	13.856		Adriatico centrale	DBMI04	50	55	4.8	
43	1908	3	17	43.000	13.300		Bolognola	POS85		55	4.6	
44	1908	11	16	43.155	13.596		Adriatico centrale	DBMI04	40		5.4	
45	1909	3	16	42.550	13.500		Pietracamela	POS85		55	4.6	
46	1911	3	26	44.061	12.507		Rimini	DBMI04	60	60	5.2	
47	1916	5	17	44.000	12.630		Alto adriatico	CFTI	80	80	5.9	
48	1916	8	16	43.970	12.670		Alto adriatico	CFTI	80	80	5.9	
49	1917	3	21	42.900	13.400		Montegallo	POS85		55	4.6	

Table 1 continued

No.	Y	M	D	Lat	Lon	H (km)	Locality	References	I_{\max}	I_o	M_{aw}	M_w
50	1917	11	5	43.506	13.586		Numana	DBMI04	65	60	5.4	
51	1920	2	10	42.900	13.500		Ascoli piceno ov.	POS85		55	4.6	
52	1921	8	28	43.120	13.253		Sarnano	DBMI04	70	70	5.1	
53	1922	6	8	43.148	13.286		Caldarola	DBMI04	65	60	5.0	
54	1922	10	11	43.700	13.450		Medio adriatico	POS85		60	4.6	
55	1923	7	12	43.200	13.300		Tolentino	POS85		60	4.8	
56	1924	1	2	43.736	13.141		Senigallia	DBMI04	75	75	5.6	
57	1928	5	30	43.706	13.122		Adriatico centrale	DBMI04	50	55	5.1	
58	1929	1	22	43.383	13.150		Apiro	POS85		60	4.8	
59	1930	8	4	43.000	13.500		Force	POS85		60	4.7	
60	1930	10	30	43.659	13.331		Senigallia	DBMI04	85	90	5.9	
61	1930	11	9	42.883	13.300		Montemonaco	POS85		55	4.6	
62	1931	6	25	43.800	13.100		Mondolfo	POS85		55	4.6	
63	1936	12	9	43.145	13.223		Caldarola	DBMI04	75	70	4.8	
64	1937	2	26	43.900	13.100		Medio Adriatico	POS85		60	4.8	
65	1937	11	22	43.833	13.083		Mondolfo	POS85		60	4.8	
66	1942	1	31	42.900	13.533		Ascoli Piceno ovest	POS85		55	4.6	
67	1943	3	25	43.074	13.584		Offida	DBMI04	60	60	5.0	
68	1943	7	31	43.714	13.223		Senigallia	DBMI04	60	55	4.6	
69	1943	10	3	42.935	13.639		Offida	DBMI04	90	85	5.8	
70	1948	1	10	43.133	13.533		Montegiorgio	POS85		55	4.6	
71	1950	9	3	42.817	13.333		Acquasanta	POS85		60	4.7	
72	1950	9	5	42.516	13.657		Gran Sasso	DBMI04	80	80	5.7	
73	1951	8	8	42.704	13.546		Monti della Laga	DBMI04	75	70	5.3	
74	1951	9	1	43.028	13.287		Sarnano	DBMI04	70	70	5.3	
75	1956	10	7	42.500	13.500		Gran sasso	POS85		60	4.8	
76	1957	11	11	43.500	13.700		Loreto	POS85		60	4.7	
77	1959	1	1	42.650	13.650		Teramo ovest	POS85		60	4.8	
78	1962	1	23	43.921	12.806		Adriatico	DBMI04	60	65	5.0	
79	1962	10	5	43.100	13.200		Polverina	POS85		55	4.6	
80	1968	1	29	43.600	13.500		Ancona	POS85		60	4.8	
81	1969	9	26	42.550	13.600		Montorio	POS85		60	4.5	
82	1972	2	4	3.720	13.440	5	Medio Adriatico (Ancona)	C73 G85 CPTI04				4.8
83	1972	2	4	43.730	13.370	5	Medio Adriatico (Ancona)	C73 G85			5.2	4.6
84	1972	2	5	43.720	13.400	10.4	Medio Adriatico (Ancona)	C73 G85				4.6
85	1972	2	6	43.710	13.430	8.3	Medio Adriatico (Ancona)	C73 G85				4.6
86	1972	6	14	43.690	13.470	3	Medio Adriatico (Ancona)	G85 CPTI04				4.8
87	1972	11	26	42.966	13.454		Montefortino	DBMI04	80	75		
88	1972	11	30	44.000	13.200		Medio adriatico	POS85			5.4	
89	1973	11	10	44.000	13.200		Medio adriatico	POS85			4.9	
90	1982	10	17	43.336	13.015		Appennino, umbro-marchigiano	CPTI04			4.8	
91	1987	7	3	43.174	13.843	5	Porto San Giorgio	R89 CPTI04			4.8	4.56

Table 1 continued

No.	Y	M	D	Lat	Lon	H (km)	Locality	References	I_{\max}	I_o	M_{aw}	M_w
<i>Located within the boundary of the Sicilian Basal Thrust Province</i>												
1	361			37.500	14.000		Sicily	CFTI	100	100	6.6	
2	1578			37.508	13.083		Sciacca	DBMI04	70	70	5.2	
3	1624	10	3	37.270	14.750		Mineo	CFTI	90	80	5.6	
4	1716	12	1	37.502	15.087		Catania	DBMI04	70	70	5.2	
5	1718	2	20	37.599	14.619		Eastern Sicily	DBMI04	65	65	5.4	
6	1727	5	8	37.500	13.000		Sicily strait	R99		60	4.8	
7	1740	6	13	37.582	12.840		Sciacca	DBMI04	75	75	5.4	
8	1817	1	14	37.508	13.083		Sciacca	R99	55	55	4.6	
9	1818	2	20	37.600	15.130		Catanese	CFTI	95	90	6.0	
10	1820	12	25	37.267	14.683		Mineo	POS85		60	4.8	
11	1823	3	27	37.931	12.329		Favignana	R99	70	70	5.2	
12	1828	5	18	37.800	12.433		Marsala	R99	70	70	5.2	
13	1831	12	16	37.500	13.083		Sciacca	BAR1897		60	4.8	
14	1846	4	22	37.502	15.087		Catania	DBMI04	55	55	4.6	
15	1876	5	25	37.817	13.300		Corleone	R99		60	4.8	
16	1878	10	4	37.266	14.691		Mineo	ABAR2000	65	65	5.0	
17	1898	11	2	37.216	14.495		Caltagirone	DBMI04	60	55	4.6	
18	1903	7	13	37.150	14.400		Niscemi	ABAR2000		55	4.6	
19	1907	4	24	37.633	13.637		Cammarata	DBMI04	55	55	4.6	
20	1909	1	2	37.233	14.500		Caltagirone	POS85		60	4.8	
21	1909	6	7	37.817	13.300		Corleone	POS85		60	4.8	
22	1909	12	3	37.900	13.100		Camporeale	R99		55	4.6	
23	1911	10	29	37.267	14.683		Mineo	POS85		55	4.6	
24	1921	7	24	37.517	15.083		Catania	POS85		60	4.8	
25	1925	8	21	37.683	14.567		Gagliano	POS85		60	4.8	
26	1927	9	22	37.700	13.900		Vallelunga	POS85		60	4.8	
27	1933	2	26	37.559	13.170		Sciacca	DBMI04	55	55	4.6	
28	1934	9	11	37.439	14.580		Madonie	DBMI04	65	65	5.0	
29	1954	11	20	37.925	13.094		S.Cipirello	R99		60	4.8	
30	1968	1	14	37.804	13.012	19	Belice Valley	A&J87				5.2
31	1968	1	14	37.676	12.966	1	Belice Valley	A&J87				5.1
32	1968	1	14	37.830	12.983	22	Belice Valley	A&J87				4.8
33	1968	1	15	37.817	13.006	34	Belice Valley	A&J87				5.2
34	1968	1	15	37.750	12.983	13	Belice Valley	A&J87				5.5
							CFTI					
35	1968	1	15	37.793	12.960	23	Belice Valley	A&J87			6.1	4.7
36	1968	1	16	37.857	12.976	36	Belice Valley	A&J87				5.2
37	1968	1	25	37.687	12.966	3	Belice Valley	A&J87				5.2
38	1968	9	1	37.800	13.000		Gibellina	POS85		55		
39	1970	12	30	37.700	12.900		Partanna	GG1974		55	4.6	
40	1972	12	27	37.600	12.967		Menfi	LS1972		55	4.8	
23	1973	9	21	37.700	13.000		S. Margherita	LS1973		60	4.6	
24	1975	6	12	37.450	14.433		Valguarnera	POS85		60	4.8	
25	1976	10	12	37.833	13.067		Gibellina	LS1976				4.6
26	1978	1	19	37.583	14.100		San Leone	LS1978				4.6
27	1981	6	7	37.670	12.470	18	Mazara	P&AL DBMI04			4.6	4.9
28	1987	2	2	37.766	14.702	27	Regalbuto	CSI			4.6	4.7
29	1999	8	30	37.532	14.638	29	Raddusa	CSI				4.9

Table 1 continued

No.	Y	M	D	Lat	Lon	H (km)	Locality	References	I_{\max}	I_o	M_{aw}	M_w
<i>Located within the boundary of the Southern Tyrrhenian Province</i>												
1	1450			38.250	14.750		Brolo	POS85		60	4.8	
2	1559	6	29	38.167	13.333		Mondello	POS85		60	4.8	
3	1562	4	6	38.167	13.333		Mondello	POS85		60	4.8	
4	1613	8	25	38.120	14.780		Naso	CFTI	90	80	5.6	
5	1661	2	25	38.167	13.250		Isola Femmine	POS85		60	4.8	
6	1686	6	13	38.167	13.250		Isola Femmine	POS85		60	4.8	
7	1726	9	1	38.120	13.350		Palermo	CFTI	85	80	5.6	
8	1736	8	16	38.010	14.175		Ciminna	DBMI04	75	75	5.5	
9	1739	5	10	38.100	14.750		Naso	CFTI	85	80	5.5	
10	1751	8		38.167	13.417		Mondello	POS85		60	4.8	
11	1823	3	5	38.000	14.100		Sicilia Settentrionale	CFTI	85	85	5.9	
12	1889	6	30	38.583	14.583		Basso Tirreno	POS85		70	5.2	
13	1889	6	30	38.583	14.583		Basso Tirreno	POS85		70	5.2	
14	1892	3	16	38.556	14.590		Alicudi	DBMI04	80	75	5.4	
15	1892	3	16	38.556	14.590		Alicudi	DBMI04	80	75	5.4	
16	1893	5	11	38.200	13.200		Punta Raisi	POS85		60	4.8	
17	1894	12	27	38.562	14.570		Filicudi	DBMI04	70	70	5.2	
18	1894	12	27	38.562	14.570		Filicudi	DBMI04	70	70	5.2	
19	1897	5	15	38.500	13.167		Basso Tirreno	POS85		60	4.8	
20	1906	3	19	38.700	13.200		Basso Tirreno	POS85		60	4.8	
21	1908	6	30	38.600	14.500		Basso Tirreno	POS85		70	5.2	
22	1910	1	25	38.700	13.200		Basso Tirreno	POS85		60	4.8	
23	1910	2	17	38.200	13.200		Punta Raisi	POS85		60	4.8	
24	1917	2	18	38.700	13.167		Basso Tirreno	POS85		60	4.8	
25	1924	11	12	38.700	13.217		Basso Tirreno	POS85		65	5.0	
26	1930	3	26	38.548	14.467		Filicudi	DBMI04	75	75	5.0	
27	1930	3	26	38.548	14.467		Filicudi	DBMI04	75	75	5.0	
28	1940	1	15	38.080	13.430		Golfo Di Palermo	CFTI	80	75	5.3	
29	1957	5	20	38.700	14.100		Basso Tirreno	POS85		60	5.2	
30	1971	2	3	38.700	14.100		Basso Tirreno	POS85			4.8	
31	1979	1	20	38.670	12.860	10	Basso Tirreno	PO06				5.2
32	1980	5	28	38.480	14.250	19	Basso Tirreno	PO06				5.7
33	1983	10	10	38.652	12.923	1	Tirreno Meridionale	CSI1.1				4.8
34	1985	8	9	38.315	13.065	25	Punta Raisi	CSI1.1				4.7
35	1998	1	17	38.400	12.900	10	Tirreno Meridionale	PO06		50		4.8
36	1998	9	14	38.460	13.600	10	Tirreno Meridionale	PO06		50		5.1
37	2002	9	6	38.380	13.700	15	Palermo	PO06	60	60		5.9
38	2002	9	27	38.440	13.690	15	Tirreno Meridionale	PO06				5.1

Merged dataset of historical and instrumental earthquakes with moment magnitude $M_w \geq 4.5$ and depth <40 km, whose epicentre is located within the boundaries of the ABT, SBT and the STC seismotectonic provinces (grey areas in Figs. 3, 5). Source of data: CPTI04 parametric catalogue (Working group CPTI 2004a), ABAR 2000 (Azzaro and Barbano 2000), A&J87 (Anderson and Jackson 1987), BAR1897 (Baratta 1897), CFTI (Boschi et al. 2000), DBMI04 (Stucchi et al. 2007), G85 (Gasparini et al. 1985), C73 (Console et al. 1973), PO06 (Pondrelli et al. 2006), POS85 (Postpischl 1985), R89 (Riguzzi et al. 1989), R99 (Rigano et al. 1999), CSI1.1 (Castello et al. 2005)

H depth from instrumental data, M_w moment magnitude derived from the moment tensor solution, M_{aw} moment magnitude derived from the macroseismic field in the case of the historical earthquakes and through a weighted average procedure which considers both the macroseismic and the instrumental information in the case of early instrumental and instrumental events (Working Group MPS 2004b)

seismicity of the last two decades (Fig. 3). We have attributed to the same province also some other historical earthquakes (Ciminna 1736 and Naso 1613 and 1739),

which are located along the eastern portion of the northern coast of Sicily and which were followed by anomalous sea waves.

Table 2 Parametric data of the focal mechanisms drawn in Fig. 3

N	Y	M	D	Lon	Lat	Depth	Strike-A	Dip-A	Rake-A	Strike-B	Dip-B	Rake-B	M_w	Ref
<i>Adriatic Basal Thrust province</i>														
1*	1972	2	4	13.4400	43.7200	5.00	216	66	-147	112	60	-27	4.8	C73/G85
2	1972	2	4	13.3700	43.7300	5.00	319	83	48	128	77	-28	4.6	C73/G85
3	1972	2	4	13.3600	43.7200	2.00	225	63	-164	222	42	171	4.3	G85
4	1972	2	5	13.4000	43.7200	10.40	246	35	-166	145	82	-55	4.6	C73/G85
5	1972	2	6	13.4300	43.7100	8.30	212	80	-143	115	54	-11	4.6	C73/G85
6	1972	6	14	13.4700	43.6900	3.00	34	70	-170	301	81	-19	4.8	G85
7*	1987	7	3	13.8430	43.1740	5.00	140	56	80	338	35	104	4.6	R89
8	1987	7	3	13.8490	43.2010	5.00	9	55	104	205	36	71	4.1	R89
9	1987	7	3	13.8680	43.2000	5.00	185	40	78	18	50	100	4.3	R89
10	1987	7	3	13.8480	43.2050	5.00	152	60	56	25	43	134	4.3	R89
11*	1987	7	5	12.1600	43.7600	10.00	294	36	55	155	61	113	4.2	G89
12*	1991	12	15	13.0670	43.6330	9.30	130	30	60	343	64	107	4.0	F&A97
13*	1995	7	23	14.0330	42.7170	19.20	99	40	60	316	56	113	4.1	F&A97
14*	2000	5	5	13.1920	44.0140	5.00	105	25	30	347	78	112	4.3	S03
15*	2000	8	1	12.4400	43.8900	18.00	212	28	42	84	72	112	4.3	P02
<i>Southern Tyrrhenian Compressional province</i>														
16*	1998	21	6	12.670	38.430	10.0	88	38	102	252	53	80	4.6	P06
17*	1998	17	1	12.900	38.400	10.0	58	29	71	260	62	100	4.8	P06
18*	1979	20	1	12.860	38.670	10.0	72	29	53	293	67	109	4.9	P06
19	1998	21	6	13.100	38.500	10.0	69	36	77	265	55	99	4.6	P06
20	1998	20	6	13.080	38.460	10.0	69	22	76	264	68	96	5.2	P06
21	1998	14	9	13.600	38.460	10.0	72	30	80	263	60	96	5.0	P06
22	2002	27	9	13.690	38.440	15.0	41	39	70	246	53	105	5.1	P06
23*	2002	6	9	13.700	38.380	15.0	26	50	40	267	60	133	5.9	P06
24	2002	10	9	13.700	38.470	15.0	71	29	126	211	67	72	4.4	P06
25	2002	28	9	13.710	38.470	15.0	79	39	103	243	52	80	4.6	P06
26	2002	2	10	13.720	38.460	15.0	33	41	59	252	56	115	4.9	P06
27	2002	6	9	13.730	38.440	15.0	252	48	126	24	53	56	4.7	P06
28	2002	20	9	13.740	38.460	16.1	46	33	77	241	58	99	4.7	P06
29*	1981	22	6	14.090	38.490	13.0	71	47	116	215	49	65	4.8	P06
30*	1980	28	5	14.250	38.480	19.1	83	43	99	252	48	82	5.7	P06
31*	1995	23	7	14.717	38.533	17.5	105	65	70	325	32	126	4.7	F&A
32*	2002	5	4	14.740	38.480	15.0	90	41	108	246	52	75	4.4	P06
33*	1988	5	6	14.670	38.420	12.0	68	35	-157	319	77	-57	4.1	Ca96
34*	1980	1	6	14.330	38.390	10.0	65	39	91	243	51	89	4.8	P06
<i>Sicilian Basal Thrust Compressional province</i>														
35*	1968	1	15	12.9830	37.7500	10.00	270	50	90	90	40	90	5.5	A&J87
36	1968	1	16	12.9760	37.8570	36.00	250	58	80	88	33	106	5.2	A&J87
37	1968	1	25	12.9660	37.6870	2.30	270	64	85	101	26	100	5.2	A&J87
38*	1981	6	7	12.4700	37.6700	18.10	48	29	48	274	69	110	4.9	P&Al
39*	1987	8	13	15.0600	37.9000	35.90	352	42	-10	89	83	-132	4.8	P&Al
40*	1992	9	27	14.6670	37.9000	23.30	60	90	40	330	50	180	4.1	F&A
41*	1995	4	11	13.9830	37.5830	8.70	170	80	30	74	60	169	4.2	F&A
42*	1995	2	10	14.9670	37.7830	20.50	85	65	10	350	81	155	4.1	F&A
43*	1988	8	13	14.9000	37.8830	26.90	213	31	161	320	80	60	3.4	N05
44*	1993	10	12	14.8440	37.8120	23.33	236	22	-153	120	80	-70	3.6	N05
45*	1995	2	10	14.9690	37.6930	10.19	210	54	32	100	65	139	3.3	N05

Table 2 continued

N	Y	M	D	Lon	Lat	Depth	Strike-A	Dip-A	Rake-A	Strike-B	Dip-B	Rake-B	M_w	Ref
46*	2000	11	20	14.9410	37.8420	23.71	270	41	102	75	50	80	3.3	N05

Events with $M_w \geq 4.0$ and depths <40 km occurred since 1968

C73 Console et al. (1973), G85 Gasparini et al. (1985), A&J87 Anderson and Jackson (1987), G89 Gasparini et al. (1989), F&A Frepoli and Amato (2000), P&AL Pondrelli et al. (2004), F&A97 Frepoli and Amato (1997), R89 Riguzzi et al. (1989), P02 Pondrelli et al. (2002), S03 Santini (2003), N05 Neri et al. (2005), P06 Pondrelli et al. (2006)

Magnitude–frequency distributions

In order to calculate a representative Gutenberg–Richter (1944) magnitude–frequency distribution for each province, we have extracted from Table 1 only the earthquakes falling within the time of completeness for magnitude classes. Plots of the seismicity rate variation with time for magnitude classes allow us to identify time period of completeness. The Marche–Adriatic dataset may be considered complete since the year 1640 ± 200 for $M_w \geq 5.5$, since 1680 ± 80 for $5.0 \leq M_w < 5.5$ and since 1860 ± 20 for $4.5 \leq M_w < 5.0$; the Sicilian dataset would be complete since 1600 ± 200 for $M_w \geq 5.5$, since 1680 ± 100 for $5.0 \leq M_w < 5.5$ and since 1820 ± 60 for $4.5 \leq M_w < 5.0$ (Table 3 and reference therein). Substantially similar completeness intervals are computed for the same areas by other authors (Working group MPS 2004b; Pace et al. 2006). In the case of seismic sequences (e.g. Ancona 1972, Belice 1968 and Palermo 2002), we have only considered the maximum magnitude event.

The G–R distributions (ABT1, SBT1 and STC1 slopes in Fig. 4) are expressed as $\log N(M) = a - bM$, where N is the number of events of a certain magnitude M per year, a is the recurrence rate of the smallest events, and b represents the proportion of small to large magnitude earthquakes and determines the slope of the curve (Kanamori and Anderson 1975; Udias 1999; Kagan 2002a, b). Because the G–R distribution is sensitive to completeness intervals and to the selected bins of magnitude classes, for each province we have also computed two other G–R slopes (ABT2, ABT3, SBT2, SBT3 and STC2, STC3 in Fig. 4) applying completeness intervals calculated by other authors (Working Group MPS 2004b; Pace et al. 2006) (Table 3) and using two bins of magnitude ($\Delta M_w = 0.1$ and $\Delta M_w = 0.23$). All the determined G–R slopes are shown in Fig. 4. They appear substantially insensitive to the completeness assumptions and to the choice of the magnitude bin. For this paper, in order to estimate quantitatively the standard deviations of the ABT1 and SBT1 slopes, we have simulated 20,000 catalogues for each province (Rhoades 1996). The catalogues were generated assuming different uncertainties ranges in the magnitude for different time periods (± 0.2 for the time period 1981–

2006, ± 0.25 for 1911–1981, ± 0.35 for 1500–1911 in Jenny et al. 2006) and different completeness intervals in the calculated error ranges. We obtained values of b equal to 1.09 ± 0.06 and of a equal to 4.56 ± 0.33 for the ABT1; of b equal to 1.10 ± 0.07 and of a equal to 4.15 ± 0.34 for the SBT1; of b equal to 1.19 ± 0.11 and a equal to 4.83 ± 0.57 for the STC1. The computed ranges of uncertainties are graphically represented by the grey areas drawn above the GR slopes in Fig. 4. The G–R slopes ABT2, SBT2, STC2 and ABT3, SBT3, STC3, which were computed assuming the completeness intervals calculated by the Working group MPS (2004b) and by Pace et al. (2006), also fall within this uncertainty range.

Other input data and associated error

The computation of the scalar seismic moment rate (\dot{M}_o), depends on the assumed a and b values of the G–R slope, the c and d constants of the moment–magnitude relation and the value assumed for the maximum magnitude. Values and standard errors in a and b have been discussed above. The c and d values have been assumed equal to 1.5 and 16.05 following Kanamori and Anderson (1975) with standard errors of 0.05 and 0.26, respectively, given by Papazachos and Kiratzi (1992). The standard error in M_{smax} was taken from the Working group CPTI (2004a). A value of $3.0 \times 10^{10} \text{ N/m}^2$ has been assumed for the rigidity modulus (Hunstad et al. 2003).

Velocity tensor computations

Applying the formulations Eq. 1–6 described in “Procedure” and using the input data discussed in “Input data”, with associated standard deviation errors, we have first computed the rate of seismic moment release (\dot{M}_o) and subsequently the strain rate ($\dot{\varepsilon}_{ij}$) and velocity tensor (U_{ij}) within the ABT, SBT and STC seismotectonic provinces (Table 4; Fig. 5). The errors involved in the evaluation of the crustal deformation using the above seismicity relationships may be significant, owing to possible restrictions on the validity of the adopted formulas, as well as to the uncertainties of the used parameters, both those depending

Table 3 Comparison of the ranges of completeness times obtained in this paper by the method of Murgaria et al. (1987) for the earthquake datasets of Table 1 with those calculated by other authors (Working Group MPS 2004b; Pace et al. 2006)

Working group CPTI (2004a)						Pace et al. (2006)				This work			
Magnitude classes	Completeness interval (year)	Magnitude classes		Completeness interval (year)		Magnitude classes		Completeness interval (year)		Magnitude classes		Completeness interval (year)	
		ABT	SBT	ABT	SBT	ABT	SBT	ABT	SBT	ABT	SBT	ABT	SBT
4.53 ± 0.115	n.e.	5.22 ± 0.115	1871	1895	5.91 ± 0.115	1700	1700	M > 6.4	1000	M ≥ 5.5	1640 ± 200	1600 ± 200	
4.76 ± 0.115	1920	5.45 ± 0.115	1700	1700	6.14 ± 0.115	1530	1530	5.0 ≤ M ≤ 6.4	1600	5.0 ≤ M < 5.5	1680 ± 80	1680 ± 100	
4.99 ± 0.115	1871	5.68 ± 0.115	1700	1700	—	—	—	4.5 ≤ M < 5.0	n.e.	4.5 ≤ M < 5.0	1860 ± 20	1820 ± 60	

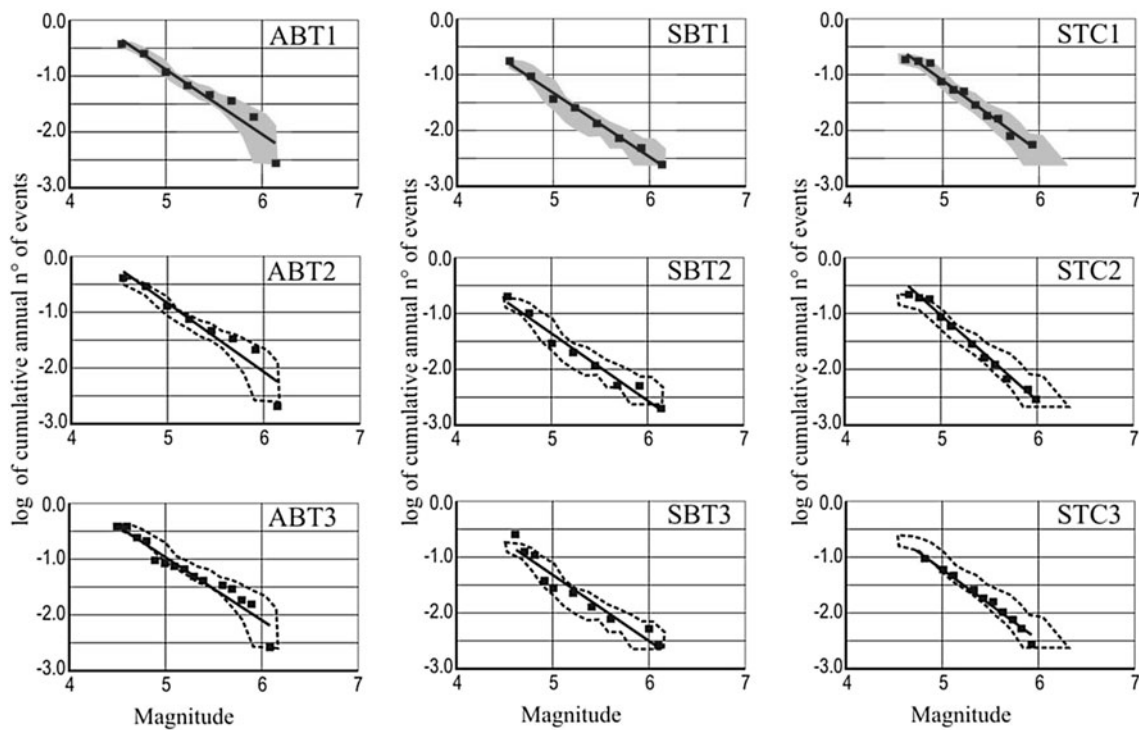
on the completeness and quality of the seismological record and those concerning the shape and size of the seismogenic volume. We have tried to evaluate the standard deviations associated with our solutions following the approach described in Papazachos and Kiratzi (1992), which allows the determination of the range of fluctuations of the results considering all the possible random errors of the model parameters by means of a generator of Gaussian noise type. Because the a , b , c and d parameters are correlated, the covariance matrix, V , is non-diagonal. Therefore, it has been necessary to compute the co-variances σ_{ab} σ_{cd} : the value of the correlation coefficient r_{ab} , calculated from our dataset, is 0.94, 0.96 and 0.84 for the ABT, SBT and STC, respectively; the r_{cd} is 0.95, as proposed by Papazachos and Kiratzi (1992). From Eq. 6, new parameters have been obtained in each iteration in order to estimate the alternative values of \dot{M}_o and the corresponding velocity tensor.

In the Table of Fig. 5, for each province, we have summarised the along-strike length (l_1), the average width (l_2) and the average thickness of the seismogenic volume (l_3), the calculated average moment rate (\dot{M}_o) and the eigenvalues of the velocity tensor ($\lambda_1, \lambda_2, \lambda_3$), measured in mm/year and the direction angles of the eigenvectors expressed as trend and plunge.

The average cumulative scalar seismic moment rates (\dot{M}_o) calculated for the ABT, SBT and STC seismotectonic provinces are 5.2×10^{23} dyne cm, 2.0×10^{23} dyne cm, 2.9×10^{23} dyne cm, respectively.

In the ABT case, the velocity tensor eigensystem has been calculated, assuming a seismogenic volume extending nearly 240 km along strike and nearly 60 km perpendicular to strike with an average thickness of 12.5 km above a basal thrust deepening westward from 0 to 25 km. The province is arcuate and convex eastward, but in the computation an average NNW–SSE strike has been assumed. Size and shape of the velocity tensor have been computed from the moment tensor (\bar{F}_{ij}) from the focal mechanism dataset in Table 2, which contains focal solutions of major and minor earthquakes. The computed shortening occurs at an average rate of 0.3 ± 0.1 mm/year along a nearly N80°E direction.

In the SBT case, the velocity tensor eigensystem has been calculated, assuming a seismogenic volume extending nearly 270 km along strike and nearly 60 km perpendicular to strike with an average thickness of 12.5 km above a basal thrust deepening northward from 0 to 25 km. The province is arcuate and convex southward, but in the computation an average E–W strike has been assumed. When the moment tensor (\bar{F}_{ij}) is computed from the entire focal mechanism dataset in Table 2, shortening at an average rate of ~ 0.1 mm/year along an average N–S direction is calculated.



SP	GR	a-value	b-value	R^2	ΔM_w	Completeness (Tab. 3)
A	ABT1	4.56±0.33	-1.09±0.06	0.94	0.23	This paper
B	ABT2	4.94	-1.15	0.94	0.23	Working Group MPS, 2004
T	ABT3	4.66	-1.13	0.93	0.1	Pace et al. 2006
S	SBT1	4.15±0.34	-1.10±0.07	0.98	0.23	This paper
B	SBT2	5.31	-1.23	0.98	0.23	Working Group MPS, 2004
T	SBT3	4.58	-1.18	0.98	0.1	Pace et al. 2006
S	STC1	4.83±0.57	-1.19±0.11	0.97	0.23	This paper
T	STC2	6.05	-1.38	0.96	0.23	Working Group MPS, 2004
C	STC3	3.80	-1.03	0.97	0.1	Pace et al. 2006

Fig. 4 Seismic potential of the Adriatic Basal Thrust (ABT), Sicilian Basal Thrust (SBT) and Southern Tyrrhenian Compressional (STC) seismotectonic province expressed as Gutenberg–Richter (G–R) slopes based on the earthquakes listed in Table 1, with exclusion of the events from the interval of catalogue completeness. For each province, three different G–R slopes were computed from the three different completeness intervals given in Table 3 and different magnitude class subdivisions ($\Delta M_w = 0.23$ from Working group

MPS 2004b and $\Delta M_w = 0.1$ from Pace et al. 2006). The grey area above the ABT1, SBT1 and STC1 slopes and the dotted areas above the other G–R slopes (ABT2, ABT3, SBT2, SBT3, STC2, STC3) represent the uncertainty range owing to errors in event magnitude and completeness length of the catalogues, as calculated in this work. The lower table reports the a value, b value and correlation coefficient (R^2) for the different computed G–R slopes

The velocity tensor eigensystem calculated for the STC seismotectonic province, assuming a rectangular parallelepiped shaped volume with a length of 260 km, surface width of 50 km, an average depth of 20 km and computing the moment tensor from the entire focal mechanism dataset in Table 2 indicate shortening at an average rate of 0.3 ± 0.1 mm/year along a N130°E direction.

For each province, the direction of the eigenvector associated with the highest absolute eigenvalue is projected in the map of Fig. 5 with a black arrow.

Discussion

In this paper, rates and azimuth of the seismic deformation which characterises the ABT province in the eastern Marche–Adriatic region, the SBT province in mainland–southern Sicily and the STC province, off the northern coast of Sicily have been obtained from seismic moment summation of the seismic activity multiplied by the moment tensor from available focal mechanisms and divided by the inferred volume of the associated

Table 4 Components of the strain rate and velocity tensors for the ABT, SBT and STC seismotectonic provinces (grey areas in Fig. 5)

Source	$\dot{\varepsilon}(11)$ ($e^{-8}/year$)	$\dot{\varepsilon}(12)$ ($e^{-8}/year$)	$\dot{\varepsilon}(13)$ ($e^{-8}/year$)	$\dot{\varepsilon}(22)$ ($e^{-8}/year$)	$\dot{\varepsilon}(23)$ ($e^{-8}/year$)	$\dot{\varepsilon}(33)$ ($e^{-8}/year$)
<i>Components of the strain tensors</i>						
ABT-P	0.01 ± 0.00	-0.01 ± 0.01	-0.05 ± 0.02	-0.20 ± 0.07	-0.06 ± 0.02	0.19 ± 0.07
ABT-W	0.02 ± 0.01	-0.03 ± 0.01	-0.11 ± 0.04	-0.40 ± 0.20	-0.11 ± 0.04	0.38 ± 0.14
SBT-P	-0.07 ± 0.03	0.00 ± 0.00	-0.01 ± 0.01	0.01 ± 0.01	0.01 ± 0.01	0.07 ± 0.03
SBT-W	-0.15 ± 0.06	0.01 ± 0.01	-0.03 ± 0.01	0.05 ± 0.02	0.03 ± 0.01	0.14 ± 0.06
STC	-0.09 ± 0.06	0.12 ± 0.08	-0.07 ± 0.05	-0.03 ± 0.02	-0.05 ± 0.04	0.11 ± 0.08
Source	U(11) (mm/year)	U(12) (mm/year)	U(13) (mm/year)	U(22) (mm/year)	U(23) (mm/year)	U(33) (mm/year)
<i>Components of the velocity tensors</i>						
ABT-P	0.03 ± 0.01	-0.02 ± 0.01	-0.03 ± 0.01	-0.12 ± 0.05	-0.03 ± 0.01	0.05 ± 0.02
ABT-W	0.06 ± 0.02	-0.03 ± 0.01	-0.03 ± 0.01	-0.24 ± 0.09	-0.03 ± 0.01	0.05 ± 0.02
SBT-P	-0.04 ± 0.02	-0.00 ± 0.00	-0.00 ± 0.00	0.01 ± 0.01	0.01 ± 0.01	0.02 ± 0.01
SBT-W	-0.09 ± 0.04	-0.01 ± 0.00	-0.01 ± 0.01	0.01 ± 0.01	0.01 ± 0.01	0.02 ± 0.01
STC	-0.04 ± 0.03	0.12 ± 0.08	-0.03 ± 0.02	-0.07 ± 0.05	-0.02 ± 0.01	0.02 ± 0.01

Positive and negative values indicate compression and tension, respectively

ABT-P Adriatic Basal Thrust-parallelepiped volume, ABT-W Adriatic Basal Thrust-wedge-shaped volume, SBT-P Sicilian Basal Thrust-parallelepiped volume, SBT-W Sicilian Basal Thrust-wedge-shaped volume, STC Southern Tyrrhenian Compressional-parallelepiped volume

seismotectonic province. The obtained results bring with them the uncertainty and the errors associated with the input data and especially with:

1. catalogue completeness and quality,
2. focal mechanism dataset,
3. attitude, size and shape of the seismogenic volume.

Uncertainties in the catalogue completeness, as well as in the reliability of the magnitude estimation, are directly involved in the magnitude–frequency distributions. For this reason, in the estimation of the Gutenberg–Richter parameters, we have considered only earthquakes with $M_w \geq 4.5$ which occurred within the time interval of catalogue completeness for classes of magnitude (Table 3). This has restricted our time of observation to the last 400 years for earthquakes with $M_w \geq 5.5$. A quantitative analysis of the range of fluctuation of the parameters of the G–R slope and of the values of magnitude has been performed with a Monte Carlo method. With such a method, all the possible random errors of the model parameters are considered by means of a generator of Gaussian noise type. On the basis of this error analysis, we consider it reasonable to assume a conservative 30% uncertainty in the estimates of the summed moment tensor. Other limits in the obtained results may be found in the calculation of the moment tensor (\bar{F}_{ij}), which is linked to the assumption for each province of an average focal mechanism.

The last, but not least, uncertainty derives from the adopted shape, size and attitude of the provinces' seismogenic volume. In order to reduce this problem as much as possible, we have neither used a subdivision in large

polygons that spans peninsular Italy and Sicily, nor adopted seismotectonic boundaries only derived from the spatial distribution and the kinematics of the seismicity, but we have adopted province boundaries which represent the surface projection of 3D homogeneous kinematic seismogenic volumes defined on the basis of integrated analysis of geological, geophysical and seismological constraints (Lavecchia et al. 2007a, b).

Any significant variation in the assumption of the surface geometry, average thickness and attitude of the seismogenic volume may strongly influence the final computational result. We have not considered any variation in the geometry of the surface boundaries, as this would also have implied a variation of the earthquakes associated with the province. The influence of the average seismogenic thickness may be interesting to consider. Let us suppose we would not have assumed for the ABT and the SBT provinces a wedge-shaped volume deepening from the surface to 25 km depth, with a consequent average thickness of 12.5 km, but we had considered a parallelepiped with an overall homogeneous thickness of 25 km, the final results in terms of maximum velocity rate would have a decrease of 50%. It is interesting to observe also that the average strike assumed for the seismotectonic province plays an important role. Variations of about 20° imply variation of about 50% in the maximum velocity rate.

In spite of the uncertainties of the input data, the obtained results show that in all three analysed seismotectonic provinces, the deformation is of the reverse-type, with prevailing sub-horizontal contractional component (λ_1), a very subordinate sub-horizontal extensional

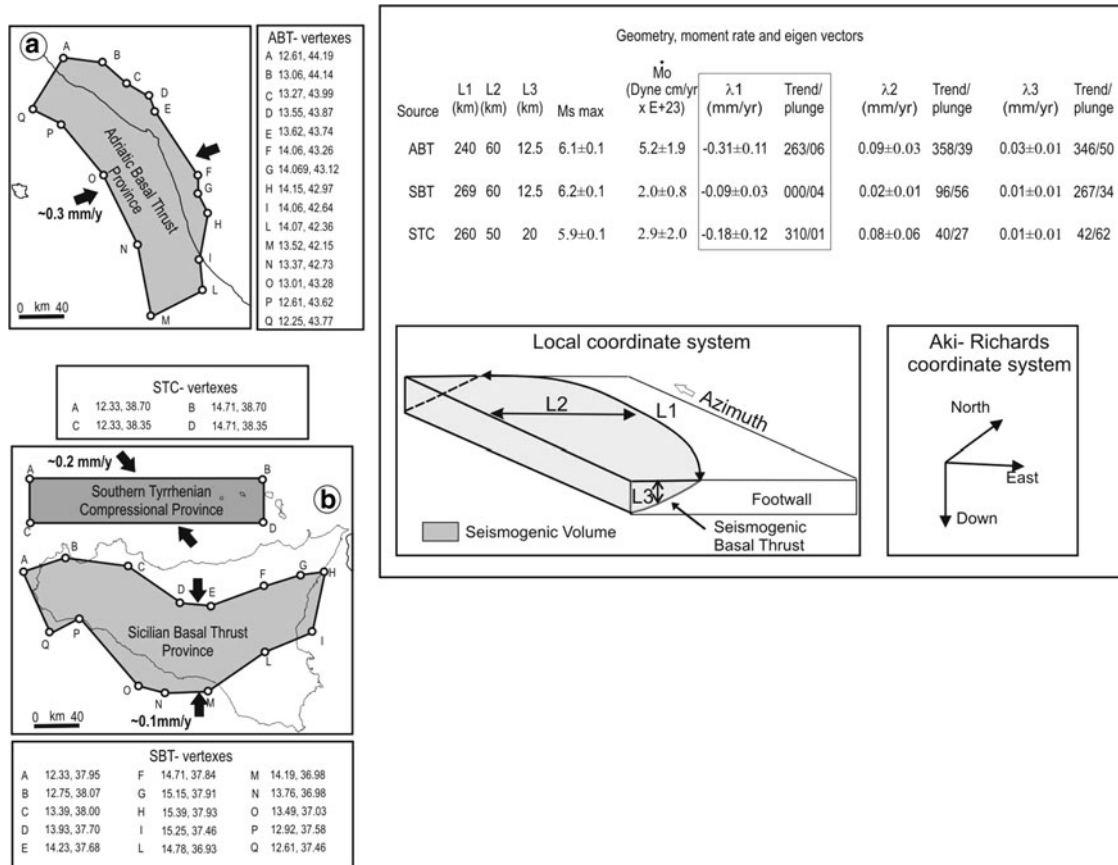


Fig. 5 Geometry and average seismic velocity tensor of the Adriatic Basal Thrust (ABT), Sicilian Basal Thrust (SBT) and Southern Tyrrhenian Compressional (STC) seismotectonic provinces. The maps report in grey the schematic area of the three provinces and the vertex of the corresponding polygons; the black arrows give the direction of the horizontal contractional component (λ_1) of the average strain tensor calculated from the focal mechanisms in Table 2. The block diagram gives a sketch of the wedge shape assumed for the ABT and SBT seismogenic volumes (L_1 length measured along-strike, L_2 surface width, L_3 average seismogenic thickness); the spatial

relationships between the local coordinate reference system and the Cartesian coordinate system, as defined by Aki and Richards (1980), are also shown. The upper table reports parameters and results of the calculation of the velocity tensors, through application of Kostrov's (1974) procedure: L_1 , L_2 and L_3 length, width and thickness of the seismogenic volume; M_{smax} = magnitude of the maximum observed event; \dot{M}_o = moment rate); λ_1 , λ_2 and λ_3 = computed eigenvectors in mm/year with trend and plunge. The lower table reports the components of the strain rate and of velocity tensors; positive and negative values indicate compression and tension, respectively

component (λ_2) and a vertical (λ_3) component. Seismic shortening happens at a rate of ~ 0.3 mm/year in an average WSW–ENE direction across the ABT province, ~ 0.1 mm/year in an average N–S direction across the SBT province and ~ 0.2 mm/year in an average NNW–SSE direction across the STC province.

In the previous literature, a SW–NE shortening rate in the range of 0.3–0.5 mm/year was computed by Westaway (1992) for the compressional regions of the northern Apennines, based on analysis of the historical earthquake record, but the eastern Marche–Adriatic region considered here had not been analysed in detail and, in any case, the strain rate and velocity tensors had not been calculated. These values were computed by Kiratzi (1994), who obtained shortening rates of 1–2 mm/year in the N–S direction across Sicily and 2–3 mm/year in the SW–NE

direction across northern Italy. No error computation was forwarded and the adopted boundaries of the seismotectonic regions were very large, and not geologically constrained. The Sicilian domain included onshore and offshore seismicity and the northern Apennine domain was also comprehensive of Padanian and Southern Alps regions. More recently, Jenny et al. (2006) have calculated distinct shortening rates for the offshore and onshore Sicilian compressional provinces, but the boundaries adopted for the zones are different from ours. In fact, they did not consider the presence of the Peloritani–Nebrodi extensional domain of northern Sicily which is interposed between mainland-southern Sicily and the Southern Tyrrhenian compressional domains. Therefore, they enlarged northward the mainland Sicily domain. In any case, their results are comparable with those obtained here,

being in the order of ~ 0.1 mm/year across mainland Sicily and ~ 0.3 mm/year across the southern Tyrrhenian belt.

In summary, the values of seismic strain rate computed in this paper substantially fit with those of Westaway (1992) and Jenny et al. (2006), but are one order of magnitude different from those of Kiratzi (1994). This may reflect different choices in the seismic catalogues and in M_s - M_o relationships, and/or in the geometry and azimuth of the estimated provinces. Furthermore, in the last 15 years, the focal mechanism dataset is greatly improved, allowing a more constrained computation of the deformation tensor. Our results are also in full agreement with those obtained by Barba et al. (2007), who applied an independent finite element modelling approach to active deformation pattern and seismotectonic sources. They calculated that the Northern Apennine region is experiencing NE-SW active compression of about 0.1–0.2 mm/year, the mainland Sicilian region is undergoing N-S shortening at rate of ~ 0.1 mm/year and the southern Tyrrhenian Sea is undergoing a N-S contraction of about 0.3 mm/year.

To compare the present seismic strain rates with the long-term geologic strain rates is difficult, because the considered seismotectonic provinces are partially (ABT and SBT provinces) or entirely (STC province) located offshore. Furthermore, in the literature there is a general lack of agreement about the tectonic style of the Apennine compressional deformation (thick-skinned vs. thin-skinned) and consequently about the long-term shortening values. Those calculated for the Umbria–Marche–Adriatic thrust belt range from ~ 10 to ~ 85 km for a time interval of ~ 12 Ma (late Miocene–early Pleistocene) (Barchi et al. 1998; Decandia et al. 1998; Finetti et al. 2001; Lavecchia et al. 2003; Basili and Barba 2007), with corresponding velocities ranging from 0.8 to 7 mm/year. Considering the only middle Pliocene–Quaternary compressional stage, which has determined the nucleation of the NE-verging fold-and-thrust structure of the outer thrust system at the hanging-wall of the ABT, a shortening in the range of 6–10 km in a time interval of nearly 2.5 Ma has been computed by Lavecchia et al. (2004), which is equivalent to shortening values of 2.5–4 mm/year. Whether this value may be extended also to the late Quaternary fold-and-thrust belt deformation is hard to decide. For some researchers, the central Apennine compression has completely ceased since Early Pleistocene times, for others it has had a progressive decrease since Miocene times, for others it has started again (since about 250,000 years) after a stop during middle Pleistocene times. The picture is still more complicated and controversial in the case of Sicily. An average southward migration rate of the late Miocene–Pleistocene compressional activity in the order of ~ 4.5 mm/year may be calculated from available

structural-kinematic maps of the region (Lavecchia et al. 2007b). A rough evaluation of the horizontal displacement accommodated by folded Quaternary terrains exposed in the Catania plain (Catalano et al. 2007) allows us to calculate shortening in the order of 0.1–0.3 mm/year. All things considered, it is evident that although the long-term geological history not only can help but is also essential for an understanding of the tectonic pattern and the style of the deforming volumes, it cannot help to definitively constrain active strain rates in these areas.

Different is the situation of the South Tyrrhenian belt where the onset of the compressional tectonics cannot be younger than early Pleistocene times. In fact, this is the age of the extensional fault structure now inverted in compression (Billi et al. 2007 and reference therein). From the data analysed in this paper, we cannot distinguish between the various kinematic interpretations proposed for the belt (north-verging or south-verging thrust), but we can observe that the associated seismic deformation budget (~ 0.2 mm/year) is similar to those across the ABT (~ 0.3 mm/year) and the SBT (~ 0.1 mm/year). This seismic budget appears especially modest given that according to geodetic data at least ~ 2 mm/year of the Africa–Nubia convergence would be accommodated across the Southern Tyrrhenian strip (Serpelloni et al. 2007). Also we wish to stress that a physical continuity between the SBT and STC provinces is obstructed by the interposition of an area in northern Sicily which is undergoing N-S extension, as clearly shown by the focal mechanism data (Fig. 1).

In general, active strain rates computed across the ABT, SBT and STC seismotectonic provinces through the analysis of geodetic data (Serpelloni et al. 2005, 2007; Jenny et al. 2006; Devoti et al. 2008; Ferranti et al. 2008) indicate velocity in the order of some mm/year that are close to the geological values, but are on average one order of magnitude higher than those obtained from seismic data. Considering that the seismic budget represents only a percentage of the overall strain, this discrepancy may imply either that a large part of the total deformation is expressed aseismically, or that the seismic deformation is underestimated owing to catalogue incompleteness and longer-term recurrence interval of strong earthquakes, or that the seismic deformation might be driven by small-scale tectonic processes. (Selvaggi 1998; Papanikolaou et al. 2005). Therefore, we cannot exclude a large amount of seismic release in the near future.

Conclusions

Historical and instrumental seismicity (last 400 year records) were used to compute the strain rate and velocity tensors in three areas of the Italian territory undergoing

active compression (eastern Marche–Adriatic region, mainland-southern Sicily and northern Sicily offshore) (Figs. 1, 3). The surface and depth geometry of the seismogenic volumes involved in the deformations were assumed from previous papers (Lavecchia et al. 2007a, b), where they had been constrained from integrated geological–seismological data.

The errors involved in the evaluation of the crustal deformation using seismicity catalogue may be significant, owing to the possible restrictions on the validity of the adopted formulas, as well as to the uncertainties of the used parameters, that include not only the completeness and quality of the seismological record, but also the adopted geometry of the seismotectonic source. The standard deviations associated with our solutions were evaluated following the approach described in Papazachos and Kiratzi (1992), which allows the determination of the range of fluctuations of the results, considering all the possible random errors of the model parameters by means of a generator of Gaussian noise type. The seismic strain rate tensor ($\dot{\varepsilon}_{ij}$) and the velocity tensor (U_{ij}) components were computed for the ABT, SBT and STC seismotectonic provinces, with the eigenvalues measured in mm/year and the direction angles of the eigenvectors expressed as trend and plunge (table within Fig. 5). In the map of Fig. 5, the direction of the eigenvector associated with the highest absolute eigenvalue (λ_1) of each province is projected and the coordinates of the vertex of the polygons, which schematise the surface geometry of each province, are given. The level of seismic activity in terms of seismic potential, expressed as G–R slope, has also been computed for the three provinces (Fig. 4), which are almost equal in terms of their mean b values (1.1–1.2) and moderately different in terms of their average a values (4.5–4.8).

In all three analysed provinces, the strain tensor is of the reverse-type, with a prevailing sub-horizontal contractional component (λ_1) and with shortening rates of 0.3–0.4 mm/year in a nearly WSW–ENE direction across the ABT province, of 0.1–0.2 mm/year in a nearly N–S direction across the SBT province and of 0.3–0.4 mm/year in the NW–SE direction across the STC province, respectively. These evaluated compressional seismic releases are modest, but tectonically controlled and not strongly different in the three regions. This is an interesting result, as in the recent literature a growing importance in active tectonic terms has been attributed to the STC belt, where most of the recent Africa–Nubia convergence would be accommodated (Goes et al. 2004; Montone et al. 2004; Pondrelli et al. 2004; Neri et al. 2005; Billi et al. 2007). Conversely, the seismicity of the eastern Marche–Adriatic region, and especially that of the mainland-southern Sicily region, has been underestimated (Kiratzi 1994; Pondrelli et al. 1995; Jenny et al. 2006; Billi et al. 2007). Conversely, similar velocity tensors

among the ABT, the SBT and the STC indicate comparable seismogenic potential to ongoing compression along the Apennine–Maghrebian thrust front, with evident implications in terms of seismic hazard implications.

References

- Aki K, Richards P (1980) Quantitative seismology. Theory and methods. Freeman, San Francisco
- Anderson H, Jackson J (1987) Active tectonics of the Adriatic region. *Geophys J R Astron Soc* 91:937–983
- Azzaro R, Barbano MS (2000) Analysis of seismicity of southeastern Sicily: proposal of a tectonic interpretation. *Ann Geofis* 43:171–188
- Azzaro R, Barbano MS, Camassi R, D'Amico S, Mostaccio A, Piangiamore G, Scarfi L (2004) The earthquake of 6 September 2002 and the seismic history of Palermo (Northern Sicily, Italy): implications for the seismic hazard assessment of the city. *J of Seismol* 8:525–543
- Baratta M (1897) Materiali per un catalogo dei fenomeni sismici avvenuti in Italia (1800–1872). *Mem Soc Geogr Ital* 7:81–164
- Barba S, Basili R, Carafa MMC (2007) Finite element modeling-derived slip rates of seismogenic sources (http://diss.rn.ingv.it/fem/S2_D3.8.html), deliverable D3.8 of Project S2 “Valutazione del potenziale sismogenetico e probabilità dei forti terremoti in Italia” INGV/DPC http://www.ingv.it/progettiSV/Progetti/Sismologici/sismologici_con_frame.htm
- Barbano MS, Bottari A, Careni P, Casentino M, Federico B, Fonte G, Lo Giudice E, Lombardo G, Patanè G (1979) Macroseismic study of the Gulf of Patti earthquake in the geostructural frame of north-eastern Sicily. *Boll Soc Geol Ital* 98:155–174 http://www.ingv.it/progettiSV/Progetti/Sismologici/sismologici_con_frame.htm
- Barchi MR, De Feyter A, Magnani MB, Minelli G, Pialli G, Sotera BM (1998) The structural style of the Umbria–Marche fold and thrust belt. *Mem Soc Geol Ital* 52:557–578
- Basili R, Barba S (2007) Migration and shortening rates in the Northern Apennines, Italy: implications for seismic hazard. *Terra Nova* 19:462–468
- Billi A, Presti D, Faccenna C, Neri G, Orecchio B (2007) Seismotectonics of the Nubia plate compressive margin in the south Tyrrhenian region, Italy: clues for subduction inception. *J Geophys Res* 112:B08302. doi:[10.1029/2006jb004837](https://doi.org/10.1029/2006jb004837)
- Boncio P, Bracone V (2008) Active stress from earthquake focal mechanisms along the Padan Adriatic side of the Northern Apennines (Italy), with considerations on stress magnitudes and pore-fluid pressure. *Tectonophysics* 299:195–210
- Boschi E, Guidoboni E, Ferrari G, Gasperini P, Mariotti D, Valensise G (2000) Catalogo dei forti terremoti in Italia dal 461 a.C. al 1997. *Ann Geofis* 43:843–868
- Caccamo D, Neri G, Sarao A, Wyss M (1996) Estimates of stress directions by inversion of earthquake fault plane solutions in Sicily. *Geophys J Int* 125:857–868
- Castello B, Selvaggi G, Chiarabba C, Amato A (2005) CSI Catalogo della sismicità italiana 1981–2002. <http://www.ingv.it/CSI/>
- Catalano S, Torrisi S, De Guidi G, Grasso G, Lanzafame G, Romagnoli G, Tortorici G, Tortorici L (2007) Sistema a pieghe tardo- quaternarie nell'area di Catania: un esempio di fronte orogenico attivo. *Rend Soc Geol Ital* 4:181–183
- Chiarabba C, Jovane L, Di Stefano R (2005) A new view of Italian seismicity using 20 years of instrumental recordings. *Tectonophysics* 395:251–268

- Console R, Peronaci F, Sonaglia A (1973) Relazione sui fenomeni sismici dell'Anconetano. *Ann Geofis* 26:3–148
- Coward MP, de Donatis M, Mazzoli S, Paltrinieri W, Wezel FC (1999) Frontal part of the Northern Apennines fold and thrust belt in the Romagna-Marche area (Italy); shallow and deep structural styles. *Tectonics* 18:559–574
- Cristofolini R, Ghisetti F, Scarpa R, Mezzani L (1985) Character of the stress field in the Calabrian Arc and Southern Apennines (Italy) as deduced by geological, seismological and volcanological information. *Tectonophysics* 117:39–58
- D'Agostino N, Selvaggi G (2004) Crustal motion along the Eurasia-Nubia plate boundary in the Calabrian Arc and Sicily and active extension in the Messina Straits from GPS measurements. *J Geophys Res* 109:B11402. doi:[10.1029/2004JB002998](https://doi.org/10.1029/2004JB002998)
- Decandia FA, Lazzarotto A, Liotta D, Cernobbi L, Nicolich R (1998) The CROP 03 traverse: insights on postcollisional evolution of Northern Apennines. *Mem Soc Geol Ital* 52:427–439
- Devoti R, Riguzzi F, Cuffaro M, Doglioni C (2008) New GPS constraints on the kinematics of the Apennines subduction. *Earth Planet Sci Lett* 273:163–174
- Di Bucci D, Mazzoli S (2002) Active tectonics of the Northern Apennines and Adria geodynamics: new data and discussion. *J Geodyn* 34:697–707
- Ferranti L, Oldow JS, D'argenio B, Catalano R, Lewis D, Marsella E, Maschio L, Pappone G, Pepe F, Sulli A (2008) Active deformation in southern Italy, Sicily and southern Sardinia from GPS velocities of the Peri-Tyrrhenian Geodetic Array (PTGA). *Boll Soc Geol Ital (Ital J Geosci)* 127:299–316
- Finetti IR, Boccaletti M, Bovini M, Del Ben A, Geletti R, Pipan M, Sani F (2001) Crustal section based on CROP seismic data across the North Tyrrhenian–Northern Apennines–Adriatic Sea. *Tectonophysics* 343:135–163
- Frepoli A, Amato A (1997) Contemporaneous extension and compression in the Northern Apennines from earthquake fault-plane solutions. *Geophys J Int* 129:368–388
- Frepoli A, Amato A (2000) Fault plane solutions of crustal earthquakes in southern Italy (1988–1995): seismotectonic implications. *Ann Geofis* 43:437–467
- Gasparini C, Iannaccone G, Scarpa R (1985) Fault-plane solutions and seismicity of the Italian Peninsula. *Tectonophysics* 117:59–78
- Gasparini C, Maramai A, Vecchi M (1989) Il terremoto del Montefeltro del 5 luglio 1987. *Atti 8 Convengo GNGTS* 6:493–501
- Goes S, Giardini D, Jenny S, Hollenstein C, Kahle HG, Geiger A (2004) A recent reorganization in the south-central Mediterranean. *Earth Planet Sci Lett* 226:335–345
- Hunstad I, Selvaggi G, D'Agostino N, England P, Clarke P, Pierozzi M (2003) Geodetic strain in peninsular Italy between 1875 and 2001. *Geophys Res Lett* 30:1181. doi:[10.1029/2002GL016447](https://doi.org/10.1029/2002GL016447)
- Jackson J, McKenzie DP (1988) The relationship between plate motion and seismic moment tensors, and the rates of active deformation in the Mediterranean and middle east. *Geophys J* 93:45–73
- Jenny S, Goes S, Giardini D, Kahle HG (2006) Seismic potential of Southern Italy. *Tectonophysics* 415:81–101
- Kagan YY (2002a) Seismic moment distribution revisited: I. Statistical results. *Geophys J Int* 148:521–542
- Kagan YY (2002b) Seismic moment distribution revisited: II. Moment conservation principle. *Geophys J Int* 149:731–754
- Kanamori H, Anderson D (1975) Theoretical basis of empirical relations in seismology. *Bull Seismol Soc Am* 65:1073–1095
- Kiratzi A (1994) Active seismic deformation in Italian peninsula and Sicily. *Ann Geofis* 37:27–45
- Kostrov VV (1974) Seismic moment and energy of earthquakes and seismic flow of rocks. *Izv Acad Sci USSR Phys Solid Earth* 1:23–44
- Lavecchia G, Brozzetti F, Barchi M, Menichetti M, Keller JVA (1994) Seismotectonic zoning in east-central Italy deduced from an analysis of the Neogene to present deformations and related stress fields. *Geol Soc Am Bull* 106:1107–1120
- Lavecchia G, Boncio P, Creati N (2003) A lithospheric-scale seismogenic thrust in Central Italy. *J Geodyn* 36:79–94
- Lavecchia G, Boncio N, Creati N, Brozzetti F (2004) Stile strutturale e significato sismogenetico del fronte compressivo padano-adriatico: dati e spunti da una revisione critica del profilo Crop 03 integrata con l'analisi di dati sismologici. *Boll Soc Geol Ital* 123:111–125
- Lavecchia G, de Nardis R, Visini F, Ferrarini F, Barbano S (2007a) Seismogenic evidence of ongoing compression in eastern-central Italy and mainland Sicily: a comparison. *Boll Soc Geol Ital (Ital J Geosci)* 126:209–222
- Lavecchia G, Ferrarini F, de Nardis R, Visini F, Barbano S (2007b) Active thrusting as a possible seismogenic source in Sicily (Southern Italy): some insights from integrated structural-kinematic and seismological data. *Tectonophysics* 44:145–167
- McKenzie DP (1972) Active tectonics of the Mediterranean region. *Geophys J R Astron Soc* 30:109–185
- Meletti C, Patacca E, Scandone P (2000) Construction of a seismotectonic model: the case of Italy. *Pure Appl Geophys* 157:11–35
- Meletti C, Galadini F, Valensise G, Stucchi M, Basili R, Barba S, Vannucci G, Boschi E (2008) A seismic source zone model for the seismic hazard assessment of the Italian territory. *Tectonophysics* 450:85–108
- Michetti AM, Brunamonte F, Serva L (1995) Paleoseismological evidence in the epicentral area of the January 1968 earthquakes, Belice, Southwestern Sicily. In: Serva L, Slemmons DB (eds) Perspectives in paleoseismology. *Assoc Eng Geologist Spec Publ* 6:127–139
- Molnar P (1979) Earthquake recurrence intervals and plate tectonics. *Bull Seismol Soc Am* 69:115–133
- Montone P, Mariucci MT, Pondrelli S, Amato A (2004) An improved stress map for Italy and surrounding regions (Central Mediterranean). *J Geophys Res* 109:B10410. doi:[10.1029/2003JB002703](https://doi.org/10.1029/2003JB002703)
- Morelli A, Pondrelli S (1998) Il terremoto del Belice del 1968. In: Poster presented at conference “Trenta anni di terremoti in Italia: dal Belice a Colfiorito”. Erice Sicily 14–18 July 1998
- Mulargia F, Gasperini P, Tinti S (1987) Contour mapping of Italian seismicity. *Tectonophysics* 142:203–216
- Neri G, Barberi G, Oliva G, Orecchio B (2005) Spatial variation of seismogenic stress orientations in Sicily, South Italy. *Phys Earth Planet In* 148:175–191
- Pace B, Peruzza L, Lavecchia G, Boncio P (2006) Layered Seismogenic Source Model and Probabilistic Seismic-Hazard Analyses in Central Italy. *Bulletin of the Seismological Society of America* 96:107–132
- Papanikolaou ID, Roberts GP, Michetti AM (2005) Fault scarps and deformation rates in Lazio–Abruzzo, Central Italy: Comparison between geological fault slip-rate and GPS data. *Tectonophysics* 408:147–176
- Papazachos CB, Kiratzi A (1992) A formulation for reliable estimation of active crustal deformation and its application to central Greece. *Geophys J Int* 111:424–432
- Parolai S, Trojani L, Monachesi G, Frapiccini M, Cattaneo M, Augliera P (2001) Hypocenter location accuracy and seismicity distribution in the Central Apennines Italy. *Journal of Seismology* 5:243–261
- Pondrelli S, Morelli A, Boschi E (1995) Seismic deformation in the Mediterranean area estimated by moment tensor summation. *Geophys J Int* 122:938–952
- Pondrelli S, Morelli A, Ekström G, Mazza S, Boschi E, Dziewonski AM (2002) European-Mediterranean regional centroid-moment tensors: 1997–2000. *Phys Earth Planet Inter* 130:71–101

- Pondrelli S, Morelli A, Ekström G (2004) European-Mediterranean regional centroid-moment tensor catalog: solutions for years 2001 and 2002. *Phys Earth Planet In* 145:127–147
- Pondrelli S, Salimbeni S, Ekström G, Morelli A, Gasperini P, Cannuccia G (2006) The Italian CMT dataset from 1977 to the present. *Phys Earth Planet Inter* 159:286–303
- Postpischl D (1985) Atlas of isoseismal maps of Italian earthquakes. CNR, P.F. Geodinamica. Quaderni della Ricerca Scientifica 114–2A
- Rhoades DA (1996) Estimation of the Gutenberg–Richter relation allowing for individual earthquake magnitude uncertainties. *Tectonophysics* 258:71–83
- Rigano R, Antichi B, Arena L, Azzaro R, Barbano MS (1999) Sismicità e zonazione sismogenetica in Sicilia occidentale. Atti 17 Convegno GNGTS, Rome, November 10–12, 1998, CD-ROM
- Riguzzi F, Tertulliani A, Gasparini C (1989) Study of the seismic sequence of Porto San Giorgio (Marche), 3 July 1987. *Il Nuovo Cimento* 12:453–467
- Roberts GP (2006) Multi-seismic cycle velocity and strain fields for an active normal fault system, central Italy. *Earth Planet Sci Lett* 251:44–51
- Roberts GP, Michetti AM (2004) Spatial and temporal variations in growth rates along active normal fault Systems: an example from Lazio-Abruzzo, central Italy. *J Struct Geol* 26:339–376
- Santini S (2003) A note on northern Marche seismicity: new focal mechanisms and seismological evidence. *Ann Geophys* 46:725–731
- Savelli D, De Donatis M, Mazzoli S, Nesci O, Tramontana M, Veneri F (2002) Evidence for Quaternary faulting in the Metauro River Basin (northern Marche Apennines). *Boll Soc Geol Ital Vol Spec* 2002(1):931–937
- Scandone P, Stucchi M (2000) La Zonazione sismogenetica ZS4 come strumento per la valutazione della pericolosità sismica. In: Le ricerche del GNDT nel campo della pericolosità sismica (1996–1999), pp 3–14, Galadini F, Meletti C, Rebez A, 2000
- Scandone P, Patacca E, Meletti C, Bellatalla M, Perilli N, Santini U (1992) Struttura geologica, evoluzione cinematica e schema sismotettonico della penisola italiana. Atti del Convegno annuale del GNDT 1:119–135
- Selvaggi G (1998) Spatial distribution of horizontal seismic strain in the Apennines from historical earthquakes. *Ann Geofis* 41:241–251
- Selvaggi G (2006) La Rete Integrata Nazionale GPS (RING) dell'INGV: una infrastruttura aperta per la ricerca scientifica. 10 Conferenza nazionale ASITA, Bolzano (Italy), 14–17 November
- Serpelloni E, Anzidei M, Baldi P, Casula G, Galvani A (2005) Crustal velocity and strain-rate fields in Italy and surrounding regions: new results from the analysis of permanent and non-permanent GPS networks. *Geophys J Int* 161:861–880
- Serpelloni E, Vannucci G, Pondrelli S, Arganani A, Casula G, Anzidei M, Baldi P, Gasperini P (2007) Kinematics of the Western Africa–Eurasia plate boundary from focal mechanisms and GPS data. *Geophys J Int* 169:1180–1200
- Stucchi M, Camassi R, Rovida A, Locati M, Ercolani E, Meletti C, Migliavacca P, Bernardini F, Azzaro R (2007) DBMI04, il database delle osservazioni macroseismiche dei terremoti italiani utilizzate per la compilazione del catalogo parametrico CPTI04. <http://emidius.mi.ingv.it/DBMI04/>
- Udias A (1999) Principles of seismology. Cambridge University Press, New York
- Vannoli P, Basili R, Valensise G (2004) New geomorphic evidence for anticlinal growth driven by blind-thrust faulting along the northern Marche coastal belt (central Italy). *J Seismol* 8:297–312
- Vespe F, Bianco G, Fermi M, Ferraro C, Nardi A, Sciarretta C (2000) The Italian GPS Fiducial Network: services and products. *J Geodyn* 30:327–336
- Visini F, Pace B, Boncio P (2008) Extensional rate budgeting: constraints from geological and seismological data in central Italy. International meeting YORSGET 2008, Abs Vol
- Wallace LM, Beavan J, McCaffrey R, Berryman K, Denys P (2007) Balancing the plate motion budget in the South Island, New Zealand using GPS, geological and seismological data. *Geophys J Int* 168:332–352
- Ward SN (1998) On the consistency of earthquake moment rates, geological fault data and space geodetic strain: the United States. *Geophys J Int* 134:172–186
- Westaway R (1992) Seismic moment summation for historical earthquakes in Italy: tectonic implications. *J Geophys Res* 97:15437–15464
- Working group CPTI (2004a) Catalogo Parametrico dei Terremoti Italiani, version 2004 (CPTI04). INGV, Bologna. <http://emidius.mi.ingv.it/CPTI/>
- Working Group MPS (2004b) Redazione della mappa di pericolosità sismica prevista dall'Ordinanza PCM del 20 marzo 2003. Rapporto Conclusivo per il Dipartimento della Protezione Civile, INGV, Milano-Roma. <http://zonesismiche.mi.ingv.it/>
- Working Group GNDT (1982) Carta Sismotettonica d'Italia. Mem Soc Geol Ital 24:491–496
- Yeats RS, Prentice CS (1996) Introduction to special section: Paleoseismology. *J Geophys Res* 101:5847–5853